

SPECTRAL ANALYSIS OF VLF/ELF SIGNALS

A Thesis Submitted
in Partial Fulfilment of the Requirements
for the Degree of
MASTER OF TECHNOLOGY

by
AMIT PRAKASH AGRAWAL

to the

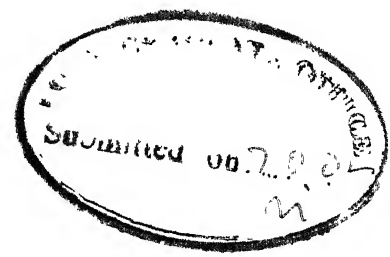
DEPARTMENT OF ELECTRICAL ENGINEERING
INDIAN INSTITUTE OF TECHNOLOGY KANPUR
AUGUST, 1982

DEDICATED
TO
MY DEAREST
ELDERS

28 MAY 1984

Doc. No. **A 82552**

EE-1982-M-AGA-SPE



CERTIFICATE

Certified that the work entitled 'SPECTRAL ANALYSIS OF VLF/ELF SIGNALS' by Mr. Amit Prakash Agrawal has been carried out under my supervision and has not been submitted elsewhere for the award of a degree.

R. Raghuram

R. Raghuram
Asstt. Professor
Department of Electrical Engineering
Indian Institute of Technology
Kanpur

ACKNOWLEDGEMENTS

I express my deep sense of gratitude and appreciation to Dr. R. Raghuram for his never flagging enthusiasm, encouragement, constructive criticism and invaluable guidance provided by him throughout the course of my thesis.

I am thankful of my friend Mr. Govind for his valuable discussions which I had with him in the hardware part of the work.

Finally I thank Mr. K.K. Misra for his efficient typing work.

AMIT P AGRAWAL

CONTENTS

	<u>Page</u>
Chapter 1 INTRODUCTION	1
Chapter 2 FAST FOURIER TRANSFORM	5
2.1 In-place algorithm	6
2.2 Signal flow graph	6
2.3 Basic properties of in-place algorithm	8
2.4 Natural input-output algorithm	9
2.5 Decimation-in-time/frequency	11
2.6 FFT algorithm for real data	11
2.7 FFT of two real functions simultaneously	12
2.8 Transform of $2N$ samples with N sample transform	12
Chapter 3 SYSTEM DESIGN CONSIDERATIONS	15
3.1 Considerations in FFT hardware implementation	15
3.2 System blocks	15
3.3 FFT processor	15
3.4 System design constraints	19
3.5 Choice of microprocessor	20
3.6 Data acquisition and display systems	23
3.7 Eight bits versus sixteen bits accuracy	25
Chapter 4 DESCRIPTION OF THE SYSTEM	29
4.1 Microprocessor kit	29
4.1.1 C.P.U.	31
4.1.2 Programmable system interface	34
4.1.3 Audio cassette interface	41
4.1.4 Memory organization	41
4.2 Data acquisition and display systems	45
4.2.1 Sample and hold	45
4.2.2 Analog to digital converter	45
4.2.3 Digital to analog converter	51

Chapter 5	SOFTWARE DESIGN	52
5.1	Selection of fixed point arithmetic	52
5.2	Scaling	53
5.3	Assembly language coding of FFT program	56
5.3.1	Initialization	56
5.3.2	Weight generation	56
5.3.3	Subroutines	59
5.3.4	Software for the data acquisition and the display systems	64
5.4	Rough estimation of execution time	64
Chapter 6	CONCLUSION AND FUTURE WORK	66
	REFERENCES	
	APPENDIX	

ABSTRACT

The objective of this project is to analyse VLF/ELF or speech signals in real time for its various frequency components using digital signal processing techniques. Fourier transform is used as a useful tool in extracting information in speech signals. Analog methods have limited resolution and flexibility. Disadvantages are overcome by taking Discrete Fourier Transform (DFT). FFT is an efficient way of realizing DFT.

The FFT is computed through the system TM 990/189 microcomputer. It consists of TMS 9980 CPU and TMS 9901 PSI (Programmable System Interface). The analog signal of low frequency is converted into digital signal which is stored in memory of the system through PSI. The output points of FFT stored in memory, are converted into analog signal and displayed on the oscilloscope. Thus the spectrum of analog signal in VLF/ELF range can be analysed.

CHAPTER 1

INTRODUCTION

Analysis of signals in the frequency domain is an important measurement concept which is widely used for providing electrical and physical system performance informations. There are many instances when signal processing involves the measurement of spectra. For example, in speech recognition problems, spectrum analysis is usually a preliminary to further acousting processing. In speech bandwidth reduction systems, spectral analysis is generally the basic measurement. In sonar systems, sophisticated spectrum analysis is required for the location of surface vessels and submarines. In radar systems, obtaining target velocity information generally implies the measurement of spectra. Thus spectrum analysis encompasses a great variety of different measurements. Several types of instruments are used for frequency response signal analysis e.g. spectrum analyser, digital Fourier analysers, wave analysers, distortion analysers and modulation analysers.

Each of the instruments measures basic properties of a signal in the frequency domain, but each uses a different technique. The Fourier analyser uses digital sampling and transformation techniques to form a Fourier spectrum display that has amplitude as well as phase information. Our project also aims at analysing the spectrum of speech or VLF/ELF signals for real time applications.

In spite of the advantages of digital signal analysis, analog methods are used for spectrum analysis at higher frequencies. The reason for this widespread use of analog methods for making this class of measurements is the ease of construction of narrow band analog filters for reasonably high frequencies. To carry out the same operation digitally the input signal must first be sampled, and then each sample is converted to its digital equivalent. If the input signal is sampled at uniformly spaced instances, the sampling rate must be at least twice the highest frequency present in the analog input signal in order to avoid errors in the measurement. The high sampling rate required by this method makes the cost of the sample and hold and ADCs which must be used in the implementation of such methods prohibitive. These requirements make the spectrum analysis increasingly difficult at higher frequencies. Our project is the spectrum analysis of speech or VLF/ELF signals.

The algorithm used for the spectrum analysis is the Fast Fourier Transform (FFT). We have selected radix-2, in-place algorithm. The processor to compute FFT can be designed using multipliers; bit-slice microprocessors or ordinary microprocessors. The design of processor with multipliers involves more hardware. In the design of processor with bit-slice microprocessors, it is a difficult to write microprogram. Therefore we chose the ordinary

microprocessors. The 16-bit TMS 9980A microprocessor was selected for our project.

To take the input samples, a data acquisition system is designed. This system samples input analog signal and converts them into digital form and are stored in the system memory. The microcomputer does the FFT and output points are displayed on the oscilloscopes. The hardware system for display is designed. The number of points and scans are displayed on the Y-axis and X-axis respectively of the oscilloscope. The magnitude of FFT points are sent to the Z-axis of oscilloscope. Thus the magnitude of spectrum can be seen in the form of intensity on the screen.

The aim of the present work is to present a compact visual display of the spectral characteristics of signals in the VLF/ELF range. Such a display enables one to readily pick out features of the signal. An application is the measurement of magnetospheric electron densities using whistlers. Whistlers are the result of the dispersion resulting from the propagation of lightening strokes or atmospherics through the magnetosphere. A spectrogram of a whistler is shown in Fig 1.1. The minimum propagation delays give the electron densities along various paths while the corresponding frequencies give the paths themselves.

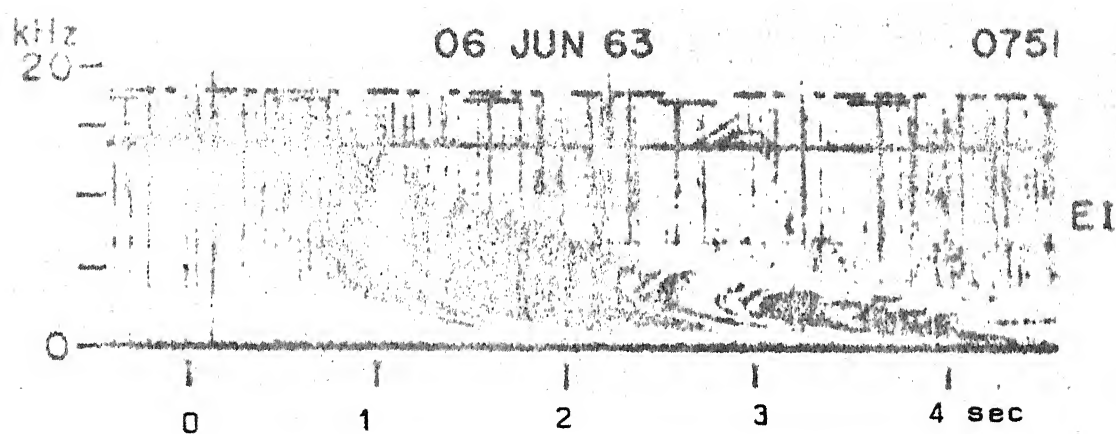


Fig 1.1 Spectrogram showing multipath whistlers recorded at eights station. The spectrogram shows several traces or components all of which originated from an atmospheric at 0 sec.

CHAPTER 2

FAST FOURIER TRANSFORM

FFT is an algorithm (i.e. a particular method of performing a series of computations) that can compute the discrete Fourier transform much more rapidly than other available algorithms. Simple calculations show that computing DFT of N complex points requires N^2 complex multiplications. The FFT owes its success to the fact that the algorithm reduces the number of multiplications and additions required in the computation of DFT.

An original algorithm developed by J.W. Cooley and J.W. Tukey reduces the computational load to $N \log_B N$ (complex multiplications), where B is the base (the base may be 2, 4, 8 or 16).

There have been some variations (like Sande-Tukey algorithm) to the original algorithm and at present there are many algorithms available for calculating the FFT. There have been many additional modifications depending on the particular requirements, the limitations of the available hardware, and the ingenuity of the individual designer or programmer.

Most of these algorithms may be classified as either (a) in place or (b) natural input-output [9]

2.1 IN PLACE ALGORITHM

An in-place algorithm is one in which a given component of any intermediate vector may be stored in the same location occupied by the corresponding component of the preceding vector. This type of algorithm requires less total storage, but at the same time the computational time is higher than that required for natural input-output algorithm. In this, either the output spectrum appears in an unnatural order or they require that the input data be arranged before entering the computation array.

Thus in-place algorithm requires the reordering of input or output data. The process in which the input points are reordered from natural to unnatural form is called scrambling. On the other hand the process in which the output points are reordered from unnatural to natural form is called unscrambling. In our system we need unscrambling operation of output points.

2.2 SIGNAL FLOW GRAPH

FFT signal flow graph for in-place algorithm for $N=8$ is shown in Fig 2.1. It consists of data array and computational arrays. Data array is represented by a vertical column of nodes on the left of the graph. The vertical columns to the right of the data array correspond to computational arrays and in general there will be r computational arrays where $r = \log_2 N$

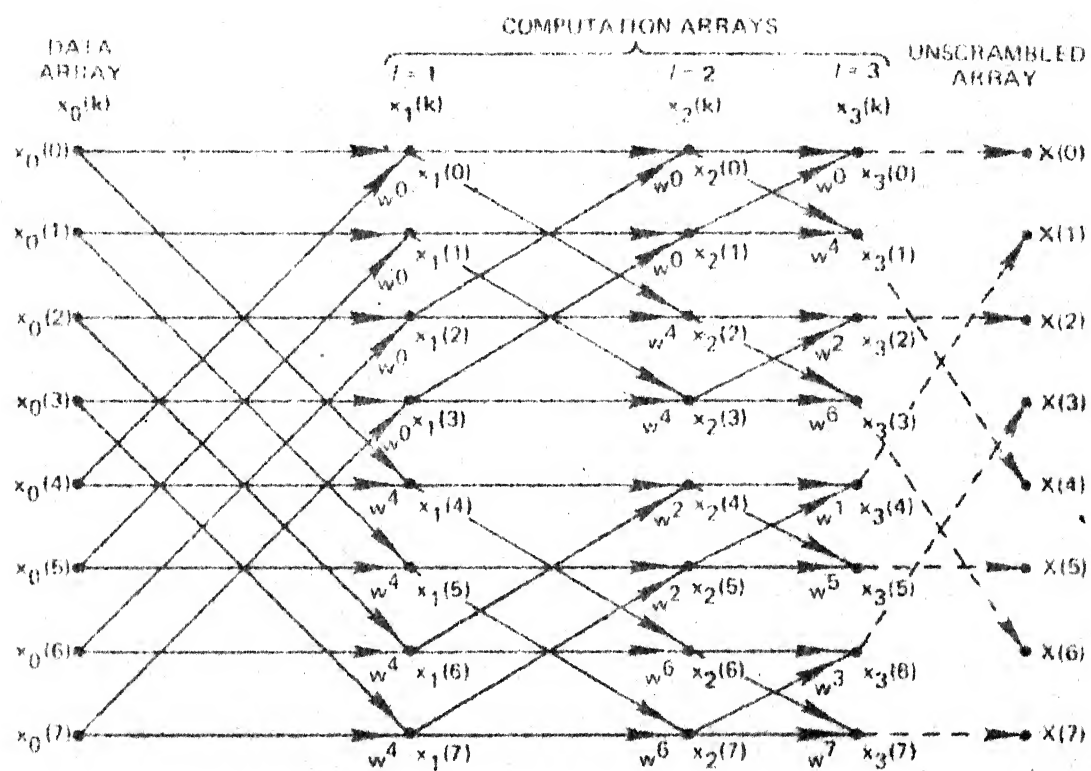


Figure 2.1 : FFT signal flow graph for $N=8$.

2.3 BASIC PROPERTIES OF IN-PLACE ALGORITHM [1]

From the flow graph, the following basic properties can be identified :

(i) Number of computational arrays

$$r = \text{Log}_2 N$$

(ii) Each array requires $\frac{N}{2}$ complex multiplications and N complex additions. Hence the total number of multiplications and additions required are $(N/2) \text{Log}_2 N$ and $N \text{Log}_2 N$ respectively. The ratio of direct to FFT computation time is

$$\frac{N^2}{N/2 \text{Log}_2 N} = \frac{2N}{\text{Log}_2 N}$$

(iii) The computation of a dual node pair requires only one multiplication and two additions. If the weighting factor at one of the nodes in a dual node pair is W^P , then the weighting factor at the other node of the pair is $W^{P+N/2}$

$$W^{P+N/2} = -W^P$$

then

$$x_{\ell}(k) = x_{\ell-1}(k) + W^P x_{\ell-1}(k + N/2)$$

$$x_{\ell}(k + N/2) = x_{\ell-1}(k) - W^P x_{\ell-1}(k + N/2)$$

here $x(k)$ indicates k^{th} component in the ℓ^{th} array.

- (iv) The spacing between dual node pairs differ from array to array. In the ℓ^{th} array ($\ell = 1, 2, \dots, r$), the spacing is $N/2$, i.e. $x(k)$ and $x(k+N/2)$ constitute a dual node pair.
- (v) To evaluate the value of P , the exponent of W , for any index in a given array, the following procedure is followed. Represent k , the node index in the ℓ^{th} array, in binary form with r bits, retain the most significant bits and add $(r-\ell)$ leading zeros to form a r bit binary number. Reverse the bit order of the resulting number. The decimal equivalent of the final binary number gives the index P . The weighting factor for the k^{th} node of the ℓ^{th} array is W^P .
- (vi) The output after r arrays is in scrambled form. To unscramble the output $x(k)$, write the index k in binary form with r bits and reverse the bit order. The resulting decimal number is the index n of $x(k)$. The unscrambling procedure is shown in Fig 2.2.

2.4 NATURAL INPUT-OUTPUT ALGORITHM

Natural input-output algorithm is one in which a given component of any intermediate vector may not be stored in the same location occupied by the corresponding component of the preceeding vector, thus requiring the extra memory for storing the intermediate result. An N point FFT

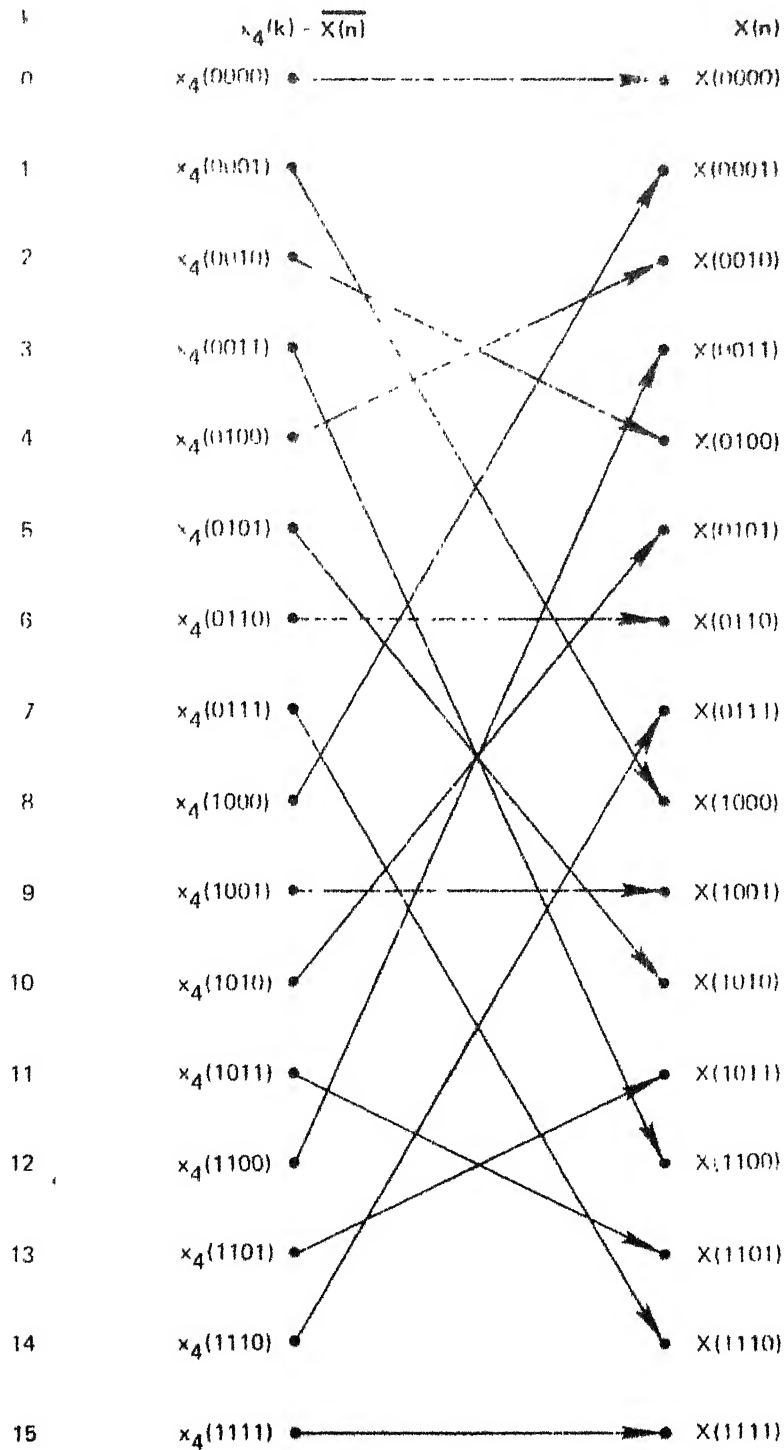


Figure 2.2 : Example of bit-reversing operation for $N = 16$.

(N real and N imaginary) will require $4N$ words of memory as compared to $2N$ words required for in-place algorithm. These algorithms, of course, maintain the natural input-output order and thus do not require scrambling/unscrambling at the input/output levels, and as such are faster as compared to the in-place algorithm. In our system, in-place algorithm has been used for it requires less number of memory locations.

2.5 DECIMATION-IN-TIME/FREQUENCY [7]

The decimation-in-time FFT algorithms are all based upon the decomposition of the DFT computation by forming smaller and smaller subsequences of the input sequence $x(k)$. Alternatively we can consider dividing the output sequence, $x(n)$, into smaller and smaller subsequences in the same manner. The class of FFT algorithms based on this procedure is commonly referred to as decimation in frequency.

2.6 FFT ALGORITHMS FOR REAL DATA [1]

In applying FFT, we often consider real function of time whereas the frequency functions are, in general complex. Thus a single computer program can be written to determine both the discrete transform and its inverse such that a complex time waveform is assumed.

If the time function being considered is real, we must set to zero the imaginary part of the complex time function.

This approach is inefficient in that the computer program will still perform the multiplications for the zero imaginary parts. In following sections two techniques for using this imaginary part of the complex time function to more efficiently compute the FFT of real functions are described.

2.7 FFT OF TWO REAL FUNCTIONS SIMULTANEOUSLY [1]

For efficient computer program, it is desired to compute the DFT of the real time functions $h(k)$ and $g(k)$ from the complex function

$$y(k) = h(k) + jg(k)$$

That is, $y(k)$ is constructed to be the sum of two real functions where one of these real functions is taken to be imaginary. After computing DFT of $y(k)$, the real and imaginary parts of the DFT are decomposed. Thus the simultaneous discrete transform of two real time functions can be accomplished.

2.8 TRANSFORM OF $2N$ SAMPLES WITH N SAMPLE TRANSFORM [1]

The imaginary part of the complex time function can also be used to compute more efficiently the DFT of a single real time function. Consider a function $x(k)$ which is described by $2N$ samples. We wish to break the $2N$ point function $x(k)$ into two N sample functions. We divide $x(k)$ as follows :

$$h(k) = x(2k)$$

$$g(k) = x(2k+1) \quad k = 0, 1, \dots, N-1$$

$$y(k) = h(k) + jg(k)$$

That is, function $h(k)$ is equal to the even numbered samples of $x(k)$, and $g(k)$ is equal to the odd numbered samples. The computation procedure is given in Fig 2.3.

A general FFT flowchart for N complex input points based on the algorithm of section 2.1 is shown in Fig 5.2. The flowchart has been implemented for our system. Since the input points are real, imaginary parts are made zero at input stage. The algorithm described in section 2.8 is more efficient for the imaginary parts of the complex time function can also be used to compute DFT of a real time function.

1. Function $x(k)$ is real $k = 0, 1, \dots, 2N-1$
2. Divide $x(k)$ into two functions

$$h(k) = x(2k) \quad k = 0, 1, \dots, N-1$$

$$g(k) = x(2k+1)$$

3. Form the complex function

$$y(k) = h(k) + jg(k) \quad k = 0, 1, \dots, N-1$$

4. Compute

$$\begin{aligned} Y(n) &= \sum_{k=0}^{N-1} y(k) e^{-j2\pi k n / N} \\ &= R(n) + jI(n) \quad n = 0, 1, \dots, N-1 \end{aligned}$$

where $R(n)$ and $I(n)$ are the real and imaginary parts of $Y(n)$, respectively.

5. Compute

$$\begin{aligned} X_r(n) &= \left[\frac{R(n)}{2} + \frac{R(N-n)}{2} \right] + \cos \frac{\pi n}{N} \left[\frac{I(n)}{2} + \frac{I(N-n)}{2} \right] \\ &\quad - \sin \frac{\pi n}{N} \left[\frac{R(n)}{2} - \frac{R(N-n)}{2} \right], n=0, 1, \dots, N-1 \end{aligned}$$

$$\begin{aligned} X_i(n) &= \left[\frac{I(n)}{2} - \frac{I(N-n)}{2} \right] - \sin \frac{\pi n}{N} \left[\frac{I(n)}{2} + \frac{I(N-n)}{2} \right] \\ &\quad - \cos \frac{\pi n}{N} \left[\frac{R(n)}{2} - \frac{R(N-n)}{2} \right], n=0, 1, \dots, N-1 \end{aligned}$$

where $X_r(n)$ and $X_i(n)$ are real and imaginary parts of $2N$ point of $x(k)$.

Fig 2.3: Computation procedure for DFT of a $2N$ point function by means of an N point transform.

CHAPTER 3

SYSTEM DESIGN CONSIDERATIONS

3.1 CONSIDERATIONS IN FFT HARDWARE IMPLEMENTATION [2]

One needs to examine the following four factors :

- (a) The reasons for building special-purpose-hardware.
- (b) What are the various options available, so far as machine organization is concerned.
- (c) Trade-offs between cost, speed and accuracy.
- (d) Interface units etc.

3.2 SYSTEM BLOCKS

The block diagram of the system is shown in Fig 3.1.

The system consists of three main blocks: (1) data aquisition system, (2) FFT processor and (3) display system.

3.3 FFT PROCESSOR [7]

The organization of an FFT processor is usually dictated by the performance and cost requirements and the technology assumed. An N -point FFT requires $\frac{N}{2} \log_2 N$ basic computations where one basic computation implies one complex multiplication, one complex addition and one complex subtraction. Depending upon the number of basic computations done in parallel, four families of machine organizations are commonly used.

(a) SEQUENTIAL PROCESSOR:

The main features of the sequential processor are :

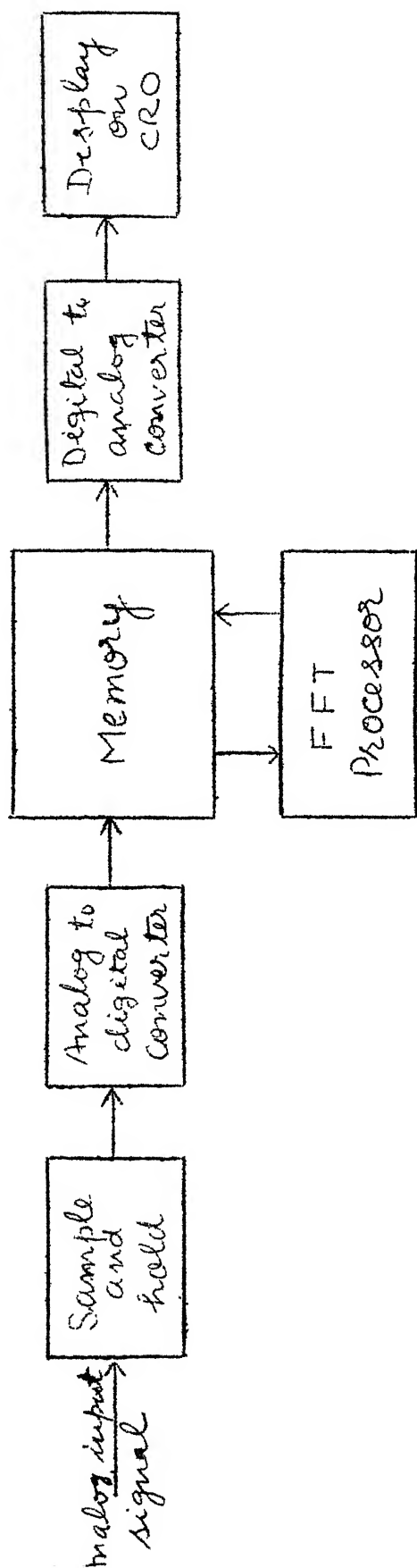


FIG 3-1: SYSTEM BLOCK DIAGRAM

- (i) One Arithmetic unit
 - (ii) $\frac{N}{2} \cdot \log_2 N$ operations sequentially.
 - (iii) Maximum sampling rate for real time processing

$$= \frac{1}{2(N-1)t} \text{ MHz, } t = \mu\text{sec, time required by a basic computation.}$$
 - (iv) Execution time = $\frac{N}{2} \cdot \log_2 N \cdot t \mu\text{sec.}$
- (b) CASCADE PROCESSOR

The sequential processor does not yield speeds generally required for real time processing of signal. Its performance can be improved by introducing a certain amount of parallelism. The main features of a cascade processor are:

- (i) $\log_2 N$ arithmetic units for $\log_2 N$ operations in parallel.
- (ii) $\frac{N}{2}$ operations sequentially.
- (iii) Maximum sampling rate allowable = $\frac{1}{t} \text{ MHz,}$
 $t = \mu\text{sec.}$

(c) THE PARALLEL ITERATIVE PROCESSOR

A second alternative for improving the performance of a sequential processor is to introduce parallelism within each iteration i.e. performing all the computations within an iteration in

parallel and $\log_2 N$ iterations sequentially. Such an organization is known as parallel iterative. The main features of this organizations are :

- (i) $\frac{N}{2}$ Arithmetic units for $\frac{N}{2}$ operations in parallel.
- (ii) $\log_2 N$ operations sequentially.
- (iii) Max. sampling rate allowable = $\frac{N}{(\log_2 N) \cdot t}$ MHz
- (iv) Execution time = $(\log_2 N) \cdot t$ μ sec.

(d) THE ARRAY ANALYSER

The organization in which $\frac{N}{2} \cdot \log_2 N$ basic computations are done in parallel is known as an array analyser. Due to high degree of parallelism, it yields a very high through-put rates. However, the cost of this approach limits its application. Its main features are :

- (i) $\frac{N}{2} \cdot \log_2 N$ a.u. for $\frac{N}{2} \cdot \log_2 N$ operations in parallel.
- (ii) Max. sampling rate allowable = $\frac{N}{t}$ MHz
- (iii) Execution time = t μ sec.

Reviewing the processors as mentioned above the sequential processor has been selected. It is slowest but cheapest. This processor can be designed with microprocessor. A microprocessor has been used because of flexibility and cost.

3.4 SYSTEM DESIGN CONSTRAINTS [8]

a) REAL TIME REQUIREMENT

Suppose we want to go upto VLF/ELF or speech signals of 5KHz, the minimum sampling rate will be 10 KHz (minimum sampling rate is double of the input signal frequency). If a 1024 point transform is chosen, a time of 0.1 sec will be available for input, processing and output for real time computation.

b) MEMORY REQUIREMENTS

- (i) Program memory
 - (ii) SINE, COS values for computation of weight
 - (iii) Values for windowing = N
 - (iv) Data memory = N or 2N depending on algorithm.
- Here N is number of sample points.

c) COMPUTATION REQUIREMENTS

- (i) $\frac{N}{2} \log_2 N$ complex multiplications or $2N \log_2 N$ real multiplications
- (ii) $N \log_2 N$ complex additions or subtraction or $2N \log_2 N$ real additions or subtraction.
- (iii) Bit reversal required for calculation of weights and for scrambling input/output depending upon the algorithm used.

d) ACCURACY:

Minimum of 16-bit processing accuracy is required. The detail is given in section 3.7.

3.5. CHOICE OF MICROPROCESSOR

An 8x8 bit multiplication sub-routine on 8080 processor takes about 200 micro-seconds. Since we are doing 16 bit processing, we will need to execute 8x8 bit sub-routine four times. So time per 16x16 bit multiplication will be 800 micro-seconds. For $\frac{N}{2} \log_2 N$ complex multiplications or $2N \log_2 N$ real multiplications, total time required will be

$$4 \times 200 \times 2 \times 1024 \times 10 = 15384 \text{ msec.}$$

Thus it is necessary to use an external fast multiplier if we want to meet the real time requirement of 0.1 sec.

In order to do one 16x16 bit multiplication on 8080 using external multiplier, 8 MOV instructions and 8 load instructions are required. Thus it will take 4000 m sec. to do $2N \log_2 N$ real multiplications. These are optimistic estimates.

The basic reason why 8080 is slow, is that we require double precision (16 bit) accuracy and 8080 is only 8 bit processor. The same problem will be with other 8 bit processors like 8085 etc. Hence it is necessary to go for a 16 bit processor. TMS 9980 microprocessor which is a 16 bit processor, has been chosen for the project. This processor has in-built multiplication routine (MPY). It does 16x16 bit unsigned multiplication.

The multiplier-interfacing to the system (TM 990/189) is not advantageous because the time taken for one multiplication by interfaced multiplier is more than that of in-built multiplication routine. One MPY instruction takes 62 cycles. The execution time for one MPY instruction can be computed [5] as follows :

$$T = t_c(\emptyset) (C+W.M)$$

where

T = total instruction time

$t_c(\emptyset)$ = clock cycle time

C = number of clock cycles for instruction execution plus address modification

W = number of required wait states per memory access for instruction execution plus address modification.

M = number of memory accesses

Here

$$t_c(\emptyset) = 0.400 \text{ micro-seconds}$$

$$C = 62$$

$$M = 10$$

$$W = 0$$

$$\begin{aligned} \text{Hence } T &= 0.400 (62 + 0.10) \\ &= 24.8 \text{ micro-seconds} \end{aligned}$$

If we interface the fast multiplier chip with the system (TM 990/189) through PSI, one LDCR and one STCR instructions

along with other instructions will be used for one multiplication. We consider only LDCR and STCR instructions. The execution time for these instructions can be computed as follows :

For LDCR; $C = 58$, $M = 6$, $W = 0$

$$\begin{aligned} T_L &= 0.400 (58 + 0.6) \\ &= 23.2 \text{ micro-seconds} \end{aligned}$$

For STCR, $C = 68$, $M = 8$, $W = 0$

$$\begin{aligned} T_S &= 0.400 (68 + 0.6) \\ &= 27.2 \text{ micro-seconds.} \end{aligned}$$

$$T = T_L + T_S = 23.2 + 27.2 = 50.4 \text{ micro-seconds}$$

Hence it can be concluded that the interfaced multiplier takes double time than that of in-built multiplier. Therefore we have used in-built multiplication routine.

3.6 DATA ACQUISITION AND DISPLAY SYSTEMS

The schemes for both the data acquisition and the display systems are shown in Fig 3.2. These schemes have been implemented and tested.

The PSI plays the key role for operating both the systems. It generates the control signals via software of the microprocessor system. The pins P8(LSB) through P15(MSB) of the PSI have been used as input output lines.

The input analog signal after sampling is digitized by analog to digital converter (ADC). The start convert pulse to ADC is generated by the monostable circuit. The trigger input to monostable is generated by pin P6 of the PSI. The EOC pulse of ADC controls the switch of the sample and hold. The outputs of ADC are latched and are read and stored in the system memory by the microprocessor. During this operation the pin P5 is high and enables the latch L1 and the buffer B2. So the display system remains off.

The microprocessor performs the FFT computations of the stored input points. The output points are again stored in the same memory locations where input sample points were stored. To display these points the pin P5 becomes low which enables the latch L2 and the buffer B3. So the data acquisition system remains off. Now the clocks at P6 goes to the counter C1. The output points appear on

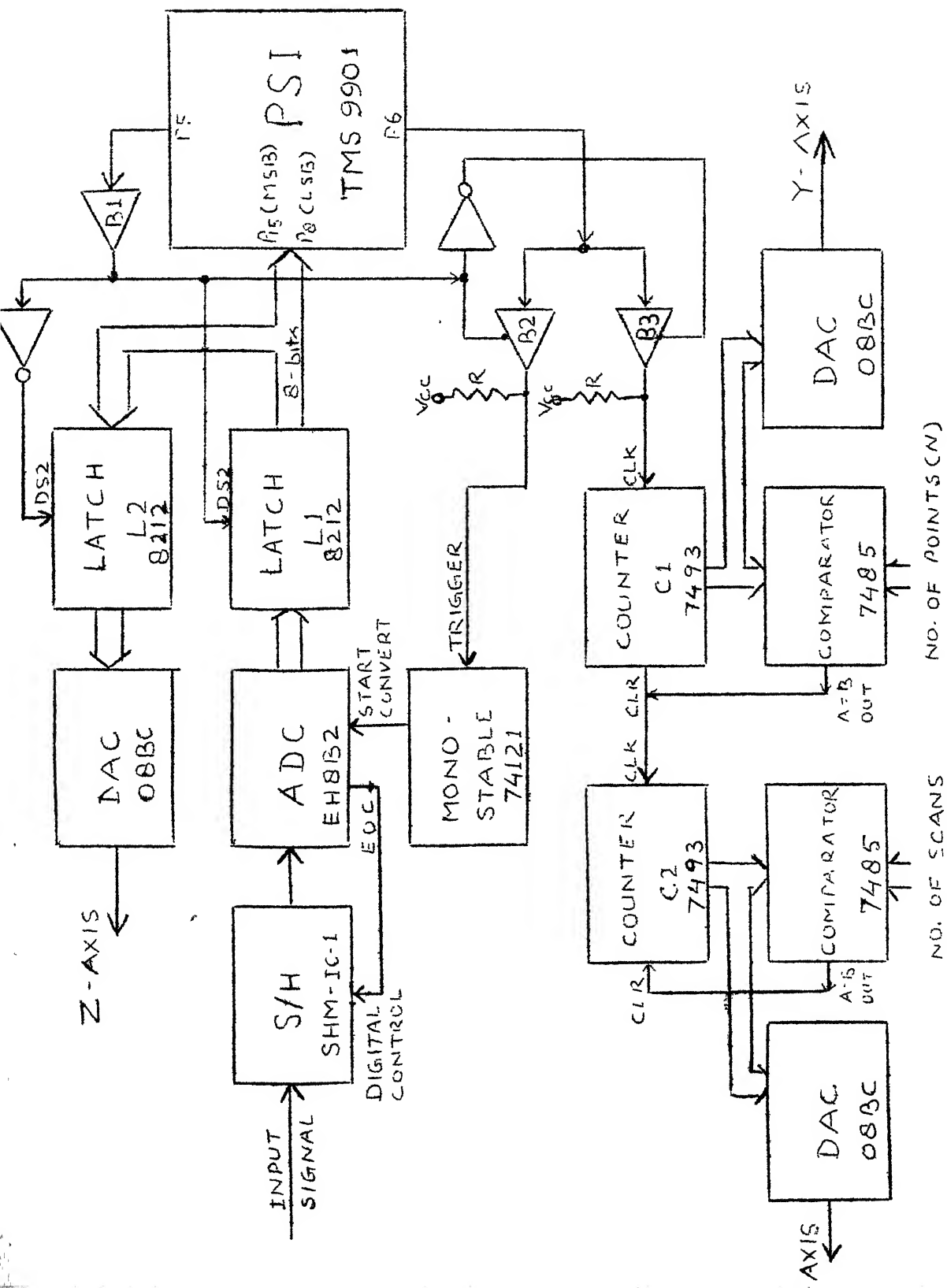


FIG 3.2 : SCHEME FOR DATA ACQUISITION AND DISPLAY SYSTEMS

the I/O pins of the PSI one by one at each clock. The 8-bit output of each FFT point is converted into analog form by digital to analog converter (DAC) and it goes to the Z-axis of the oscilloscope. At the same time the output of the counter C1 through DAC is displayed on the Y-axis of the oscilloscope. Since there is no clock to the counter C2, the output that goes to the X-axis of the oscilloscope is zero. Since the FFT computation is only for $N=32$, one clock appears at the counter C2 after the display of one set of 32 FFT points. This clock will shift the beam point right on the X-axis and the same operation is repeated and the second set of FFT points are displayed on the screen and so on. The intensity on the Y-axis displays the magnitude of the FFT points.

The timing diagrams for the data acquisition and the display systems are shown in Fig 3.3(a) and 3.3(b). The chapter four and five describe respectively the hardware and software part of the data acquisition and the display systems.

3.7 EIGHT BITS VERSUS SIXTEEN BITS ACCURACY

With 8 bits in fractional part the precision of 8 bits is given by

$$\text{Precision (8 bits)} = 8 \times \log_{10} 2 = 2.41 \text{ digits}$$

By increasing the number of bits in the fractional part a more accurate representation for the spectrum can

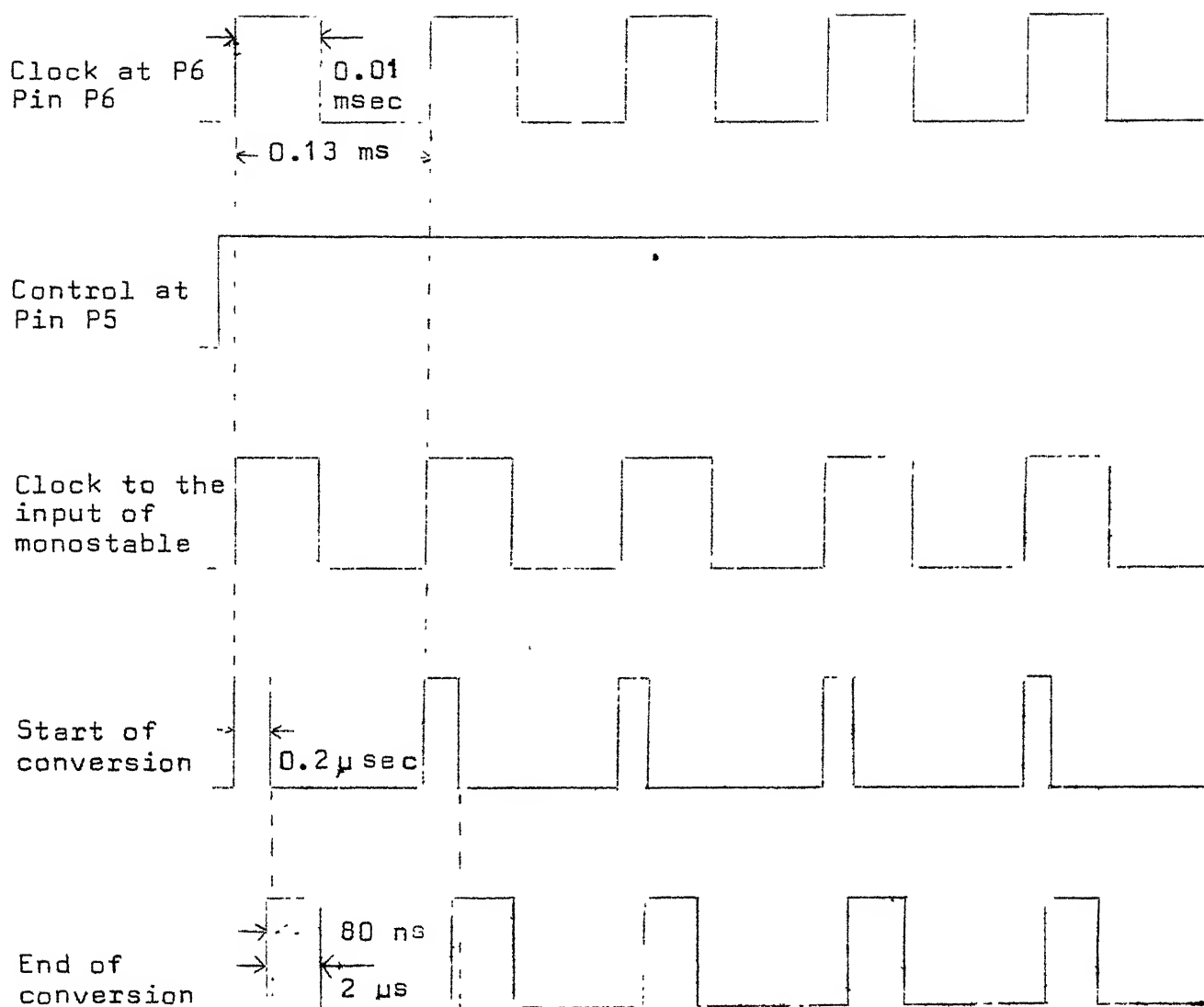


Fig 3.3(a) Timing diagram of the Data Acquisition System

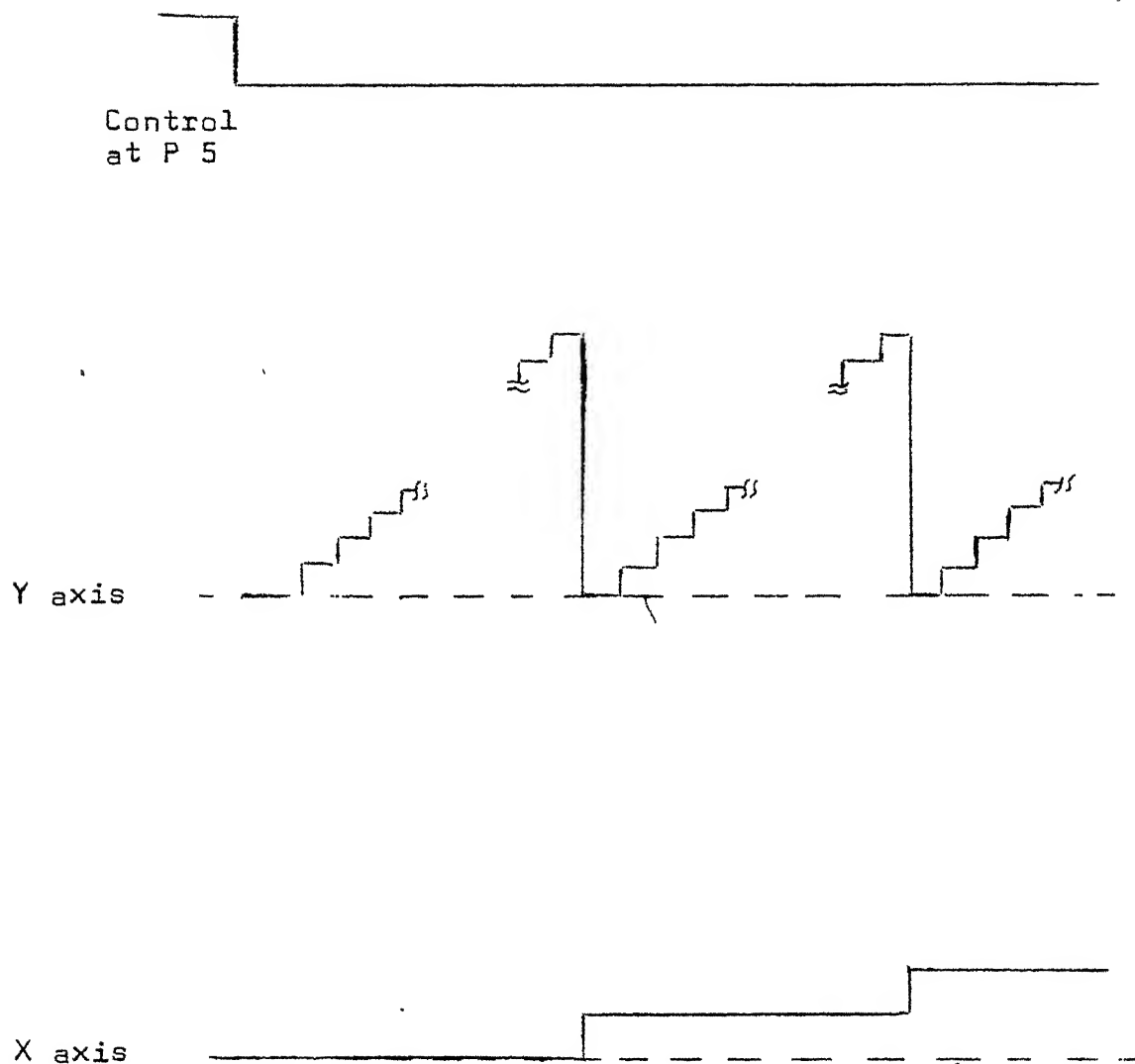


Fig. 3.3(b) Timing diagram for display system

be obtained. Also computation time considerations dictate that the maximum number of bits be limited. With 16 bits, sufficient accuracy of representation can be obtained without degrading the computation time to a large extent.

With 16 bits, precision of 16 bits can be calculated as

$$\text{Precision (16 bits)} = 16 \times \log_{10} 2 = 4.82 \text{ digits}$$

This is quite sufficient for the envisaged use. Therefore 16 bits accuracy for the computation of FFT has been chosen for our project.

CHAPTER 4

DESCRIPTION OF THE SYSTEM

4.1 MICROPROCESSOR KIT

The system used is Texas Instruments TM 990/189 [5]. It is a self-contained, single-board microcomputer system. The system features include:

- TMS 9980A microprocessor.
- 1024 bytes of RAM expandable on board to 2048
- Bytes (each byte contains 8 bits of data)
- 4096 bytes of ROM expandable on board to 6144 bytes
- 2 MHz crystal controlled clock
- Audio cassette interface
- 16 bit programmable I/O port and interrupt monitor (TMS 9901)
- 45 - key alphanumeric keyboard
- Ten-digit, seven-segment L.E.D. type alphanumeric display
- Visual and acoustic indicators
- Resident system monitor and assembler
- Single step instruction execution

In addition to onboard memory expansion, two other system expansion options are available :

- A TMS 9902 asynchronous communications controller, and accompanying interface circuits for either RS-232-C or 20 mA current loop terminals can be added.

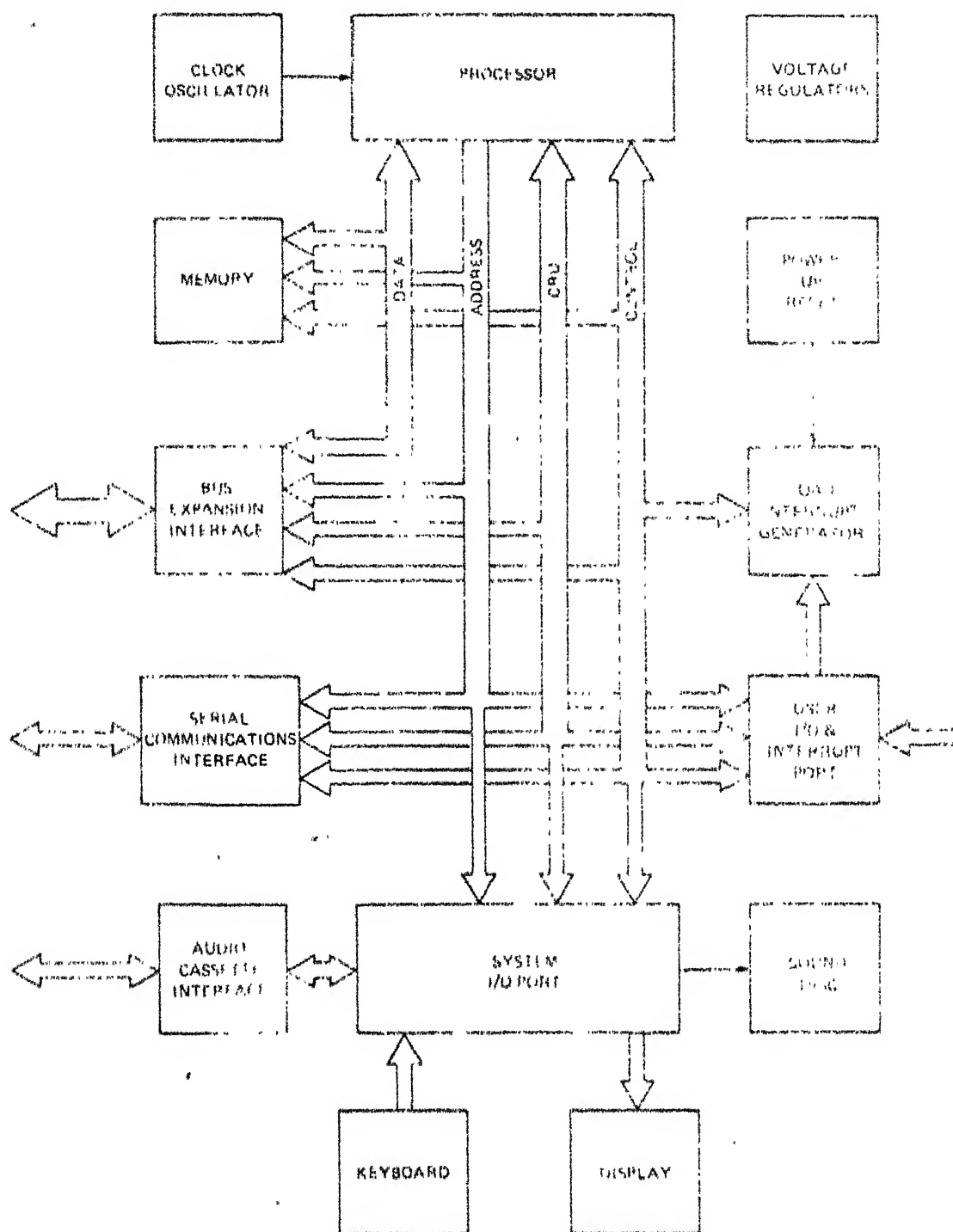


Figure 4-1: System Block Diagram

- The bus can be expanded by use of the Bus Interface.

Figure 4.1 shows the system architecture along with the user options.

4.1.1. C.P.U.

The TMS 9980A is a software-compatible member of TI's 9900 family of microprocessors. The key features are:

- 16 Bit Instruction word
- Full Minicomputer Instruction Set Capability Including Multiply and Divide (multiplication and division)
- Upto 16,384 Bytes of Memory
- 8 Bit memory data bus
- Advanced Memory to Memory Architecture
- Separate Memory, I/O, and Interrupt. Bus Structures
- 16 General Registers
- 4 Prioritized Interrupts
- Programmed and DMA I/O capability
- On-chip 4 phase clock Generator
- 40 pin package
- N-Channel Silicon-Gate Technology

A word is defined as 16 bits or 2 consecutive bytes in memory. The words are restricted to be on even address boundaries, i.e. the most significant half (8 bits) resides at even address and the least significant half at the subsequent odd address. A byte can reside at even or odd address.

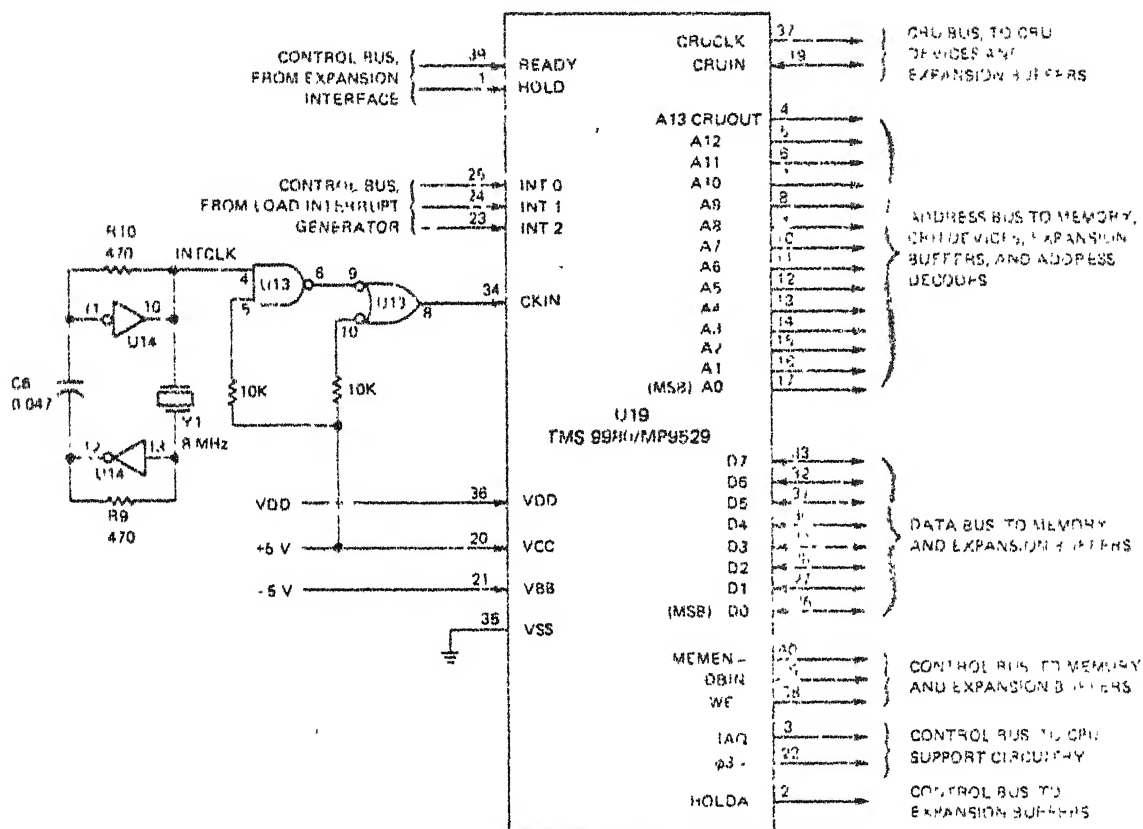


Figure 4-2 TMS 9980A Signals

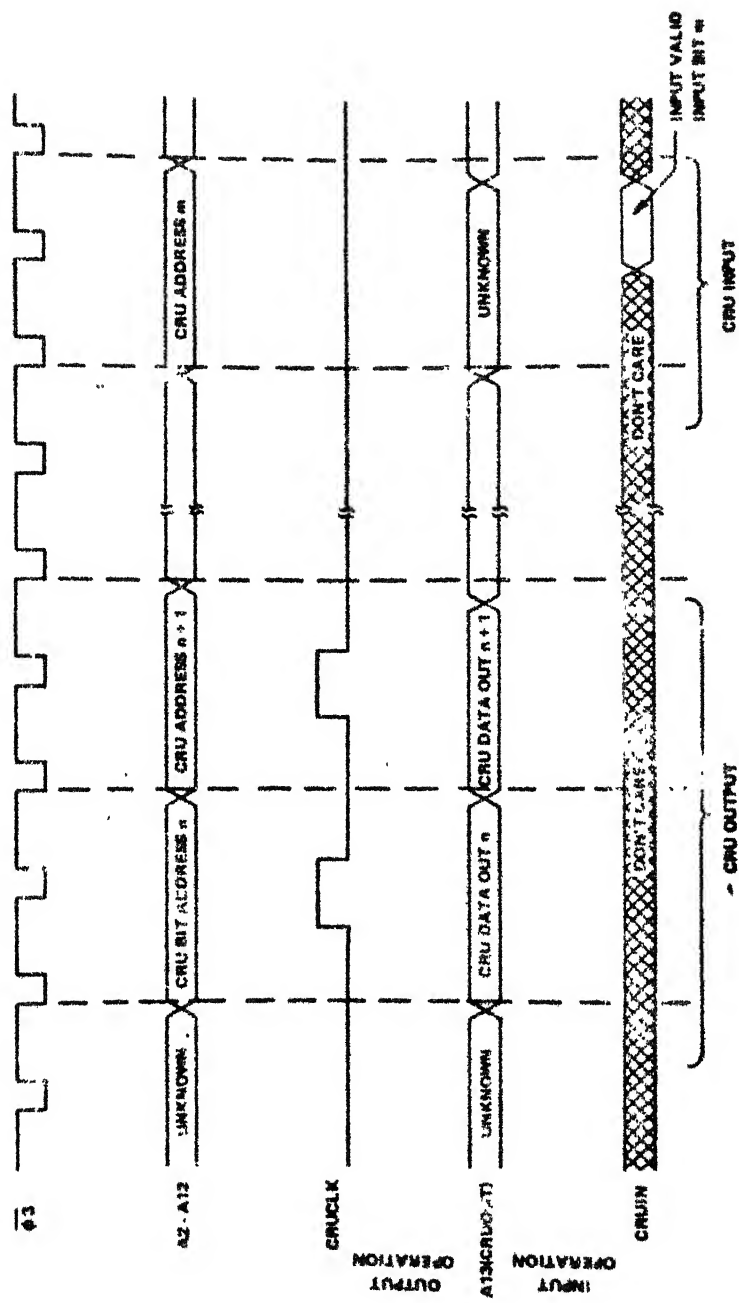


FIGURE 4-3- THE 8000A/THE 9001 CRU INTERFACE TIMING

The microprocessor signals are shown in Fig 4.2. The TMS 9980A CRU Interface Timing is shown in Fig 4.3.

4.1.2 PROGRAMMABLE SYSTEM INTERFACE (PSI)

It is a multifunctional component designed to provide low cost interrupt and I/O ports and an interval timer for TMS 9900 - family microprocessor systems. The key features are :

- 9900 - family peripheral
- Performs interrupt and I/O Interface functions:
 - (i) Six dedicated interrupt lines
 - (ii) Seven dedicated I/O lines
 - (iii) Nine programmable lines as I/O or interrupt
 - (iv) Up to 15 interrupt lines
 - (v) Up to 22 input lines
 - (vi) Up to 16 output lines
- Easily cascaded for expansion
- Interval or Event Timer
- Single 5v power supply
- All inputs and outputs TTL-Compatible

The TMS 9901 Pin assignments and functions are shown in Fig 4.4. The TMS 9901 can be divided into three sub-systems: CRU interface, input/output interface and interrupt interface.

a) CRU INTERFACE

The CPU communicates with the TMS 9901 PSI via the CRU. The typical TMS 9901 application is shown in Fig 4.5. The

SIGNATURE	PIN	I/O	DESCRIPTION
INTREQ	11	OUT	<p>INTERRUPT Request. When active (low) INTREQ indicates that an enabled interrupt has been received. INTREQ will stay active until all enabled interrupt inputs are removed.</p>
IC0 (MSB)	15	OUT	Interrupt Code lines. IC0-IC3 output the binary code corresponding to the highest priority enabled interrupt. If no enabled interrupts are active IC0-IC3 = (1,1,1,1).
IC1	14	OUT	
IC2	13	OUT	
IC3 (LSB)	12	OUT	
CE	5	IN	<p>Chip Enable. When active (low) data may be transferred through the CRU interface to the CPU. CE has no effect on the interrupt control section.</p>
S0	39	IN	Address select lines. The data bit being accessed by the CRU interface is specified by the 5-bit code appearing on S0-S4.
S1	36	IN	
S2	35	IN	
S3	25	IN	
S4	24	IN	
CRUIN	4	OUT	<p>CRU data in (to CPU). Data specified by S0-S4 is transmitted to the CPU by CRUIN. When CE is not active CRUIN is in a high-impedance state.</p>
CRUOUT	2	IN	<p>CRU data out (from CPU). When CE is active, data present on the CRUOUT input will be sampled during CRUCLK and written into the command bit specified by S0-S4.</p>
CRUCLK	3	IN	<p>CRU Clock (from CPU). CRUCLK specifies that valid data is present on the CRUOUT line.</p>
RST1	1	IN	<p>Power Up Reset. When active (low) RST1 resets all interrupt masks to "0", resets IC0 - IC3 = (0, 0, 0, 0). INTERQ = 1, disables the clock, and programs all I/O ports to inputs. RST1 has a Schmitt-trigger input to allow implementation with an RC circuit as shown in Figure 7.</p>
VCC	40		Supply Voltage +5 V nominal.
VSS	16		Ground Reference
ϕ	10	IN	System clock (ϕ 3 in TMS 9900 system, CKOUT in TMS 9980 system).
INT1	17	IN	<p>Group 1, interrupt inputs</p> <p>When active (Low) the signal is ANDed with its corresponding mask bit and if enabled sent to the interrupt control section. INT1 has highest priority.</p>
INT2	18	IN	
INT3	9	IN	
INT4	8	IN	
INT5	7	IN	
INT6	6	IN	
INT7/P15	34	I/O	<p>Group 2, programmable interrupt (active low) or I/O pins (true logic). Each pin is individually programmable as an interrupt, an input port, or an output port.</p>
INT8/P14	33	I/O	
INT9/P13	32	I/O	
INT10/P12	31	I/O	
INT11/P11	30	I/O	
INT12/P10	29	I/O	
INT13/P9	28	I/O	
INT14/P8	27	I/O	
INT15/P7	23	I/O	
P0	38	I/O	<p>Group 3, I/O ports (true logic): Each pin is individually programmable as an input port or an output port.</p>
P1	37	I/O	
P2	26	I/O	
P3	22	I/O	
P4	21	I/O	
P5	20	I/O	
P6	19	I/O	

Fig 4.4 TMS 9901 Pin Assignments and Functions

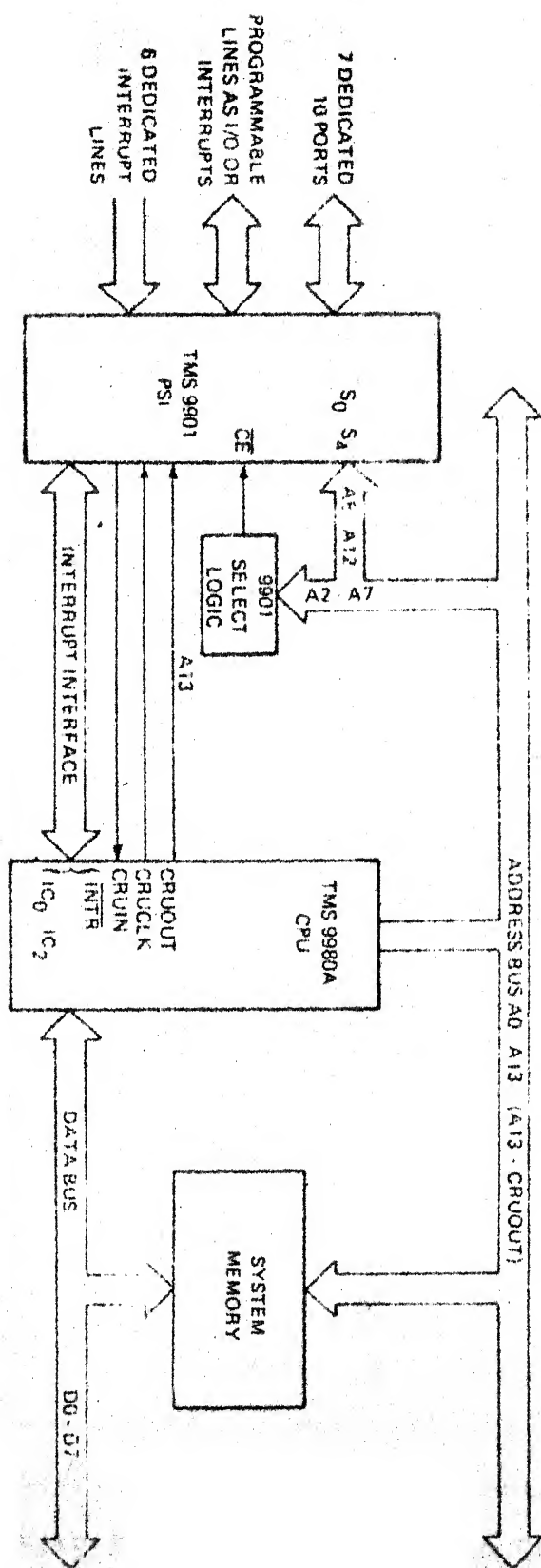


Figure 4-5: Typical TMS 9901 Programmable System Interface (PSI) Application

TMS 9901 occupies 32 bits in CRU read space and 32 bits in CRU write space. The Table 4.1 shows the mapping for CRU bit addresses to TMS 9901 function. The CRU interface consists of five address select lines (S0-S4), chip enable (\overline{CE}) and the three CRU lines (CRUIN, CRUOUT, CRUCLK). In the case of a write operation, the TMS 9901 strobes data off the CRUOUT line with CRUCLK. For a read operation, the data is sent to CPU on CRUIN line. The chip enable is generated by decoding the high-order address bits (A0-A9) on CRU cycles.

CRU is a bit addressable (4096 bits), synchronous, serial interface over which a single instruction can transfer between one and 16 bits serially. Each one of the 4096 bits of the CRU space has a unique address and can be read and written. During multi-bit CRU transfers, the CRU address is incremented at the beginning of each CRU cycle to point to the next consecutive CRU bit. When a 9980 CPU executes a CRU instruction, the processor uses the contents of workspace register 12 as a base address. The CRU address is brought out on the 15-bit address bus; this means that the least significant bit of R12 is not brought out of the CPU. During CRU cycles, the memory control lines (\overline{MEMEN} , \overline{WE} and DBIN) are all inactive; \overline{MEMEN} being inactive (High) indicates the address is not a memory address and therefore is a CRU address or external instruction code. Also when \overline{MEMEN} is inactive (High) and a valid address is present, address bits A0-A2 must all be zero to constitute a valid CRU address.

b) INPUT/OUTPUT INTERFACE

Upto 16 individually controlled, I/O lines are available and the unused dedicated interrupt lines also can be used as input lines. After reset all I/O lines are programmed as inputs. By writing to any I/O line, that line will be programmed as an output line until another reset occurs. An output line can be read and indicates the present state of the pin. A pin programmed to the output mode can not be used as an input pin. Applying an input current to an output pin may cause damage to the TMS 9901. The TMS 9901 outputs are latched and buffered off chip, and inputs are buffered onto the chip.

c) PROGRAMMABLE PORTS

A total of nine pins ($\overline{\text{INT7/P15}}-\overline{\text{INT15/P7}}$) on the TMS 9901 are user-programmable as either I/O lines or interrupts. Any pin which is not being used for interrupt should have the appropriate interrupt mask disabled ($\text{mask}=0$) to avoid erroneous interrupts to the CPU. To program one of the pins as an interrupt, its interrupt mask simply is enabled and the line may be used as if it were one of the dedicated interrupt lines.

d) SOFTWARE INTERFACE

Figure 4.6 lists the TMS 9980 code needed to control the TMS 9901 PSI. The code initializes the PSI to an eight-bit input port, and an eight bit output port.

ASSUMPTION:

- System uses clock at maximum interval (349 msec @ 3MHz)
- Interrupts 1-6 are used
- Eight bits are used as an output port, P0 - P7
- Eight bits are used as an input port, P8 - P15
- RST1 (power-up reset) has been applied
- The most significant byte of R1 contains data to be output.

LI	R12, PSIBAS	Set up CRU base to point to 9901
LDCR	@CLKSET, 0	16-bit transfer, set clock to max interval
LDCR	@INTSET, 7	Enter interrupt mode and enable interrupts 1 - 6
LI	R12, PSIBAS+32	Set CRU base to I/O ports - output
LDCR	R1, 8	Output byte from R1, program ports 0 - 7 as output
LI	R12, PSIBAS+48	Set CRU base to I/O ports - input
STCR	R2, 8	Store a byte from input port into MSBT of R2
LI	R12, PSIBAS	Set CRU base to 9901
SBZ	0	Leave clock mode so decremented contents can be latched
INCT	R12	Set CRU base to clock read register
SBO	-1	Enter clock mode
STCR	R3, 14	Read 14-bit clock read register contents into R3
CLKSET	DATA	>FFFF
INTSET	BYTE	>7E
CLKINT	\$	Clock interrupt service routine - level 3
	LIMI	0
	INC	@COUNT
	LI	R12, PSIBAS
	SBZ	0
	SBO	3
		Disable interrupts at CPU
		Count the clock interrupt
		Set CRU base to point to 9901
		Enter interrupt mode
		Clear clock interrupt

FIGURE 4.6 TMS 9980 SAMPLE SOFTWARE TO CONTROL THE TMS 9901

Fig 4.6 TMS 9980 Sample Software to Control the TMS 9901

e) USER I/O PORT

The detailed discription of the user I/O Port is shown in Fig 4.7. The user I/O Port extends from R12 CRU address 000_{16} to $03E_{16}$. The low order four bits (R12 CRU addresses 020 through 026) are also connected to the drivers for light emitting diodes CR1 through CR4 which illuminate in response to a logic one input. The individual bit assignments of the User Port are shown in Table 4.2.

4.1.3 AUDIO CASSETTE INTERFACE (ACI)

An audio cassette recorder can be used as a storage medium for programs used with the TM 990/189. Figure 4.8(a) shows the location of the pins for audio in, audio out and motor control. Figure 4.8(b) indicates the recorder and ACI connections. To dump memory to the cassette, the following instruction is used.

```
' D <start address> <Sp> <stop address> <Sp>
  <entry address> <Sp> IDT= <name> <Sp> READY <Y>'
```

To load the memory from the cassette, L command is used.

4.1.4 MEMORY ORGANIZATION

With fourteen address lines, the TMS 9980A can address upto 16,384 eight bit memory locations. In this system, a total of 8192 locations are dedicated to onboard devices and the remaining locations are reserved for off-board functions. The off-board memory expansion capability is

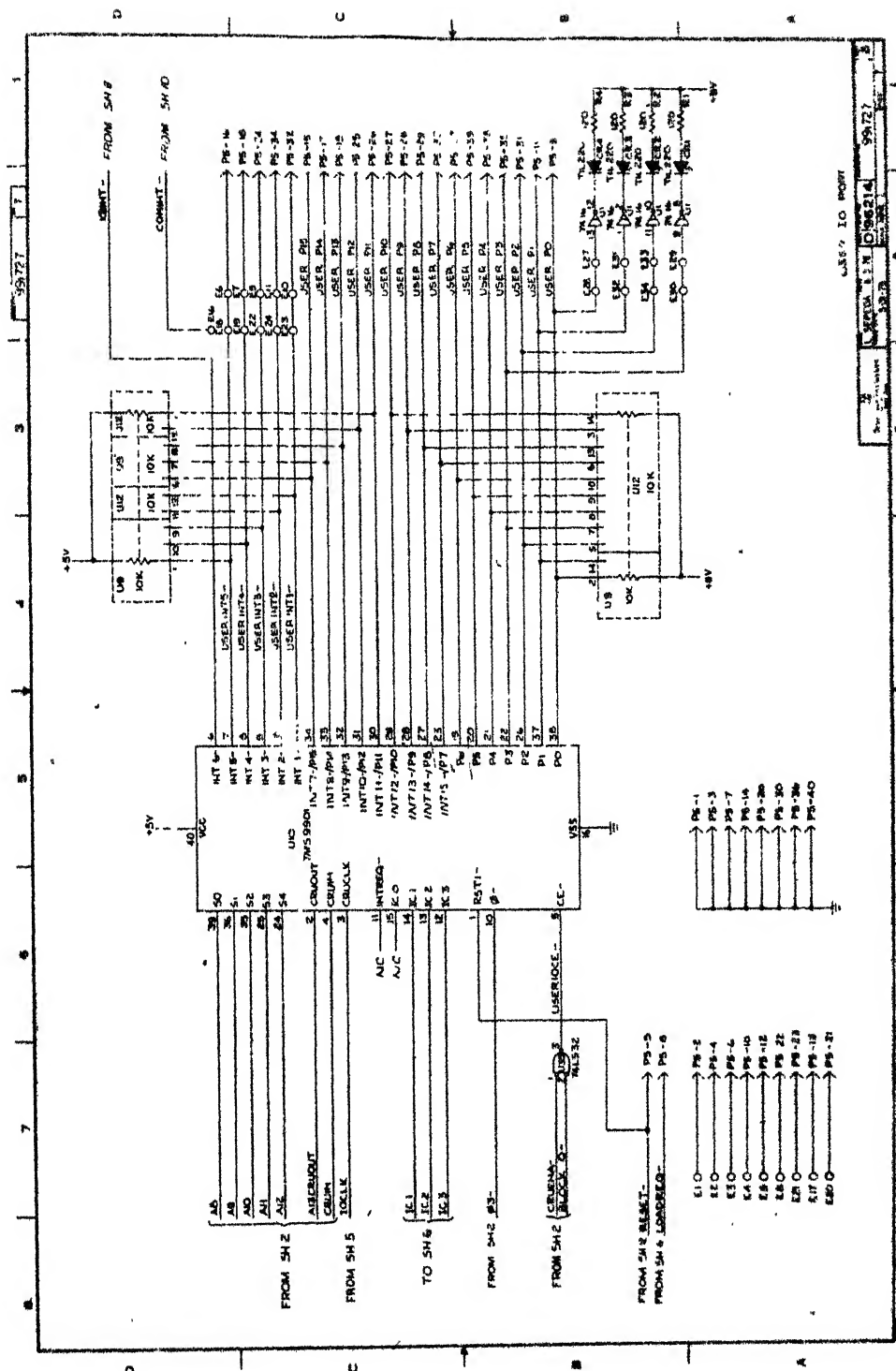


TABLE 8-2 USER PORT I/O MAP

CPU ADDRESS	TMS 9901 BIT ASSIGNMENT			SIGNAL LINE AFFECTED
	BIT ADDRESS	INPUT	OUTPUT	
000	0	CONTROL BIT	CONTROL BIT	
001	1	INT1--, CLK 1	MASK 1, CLK 1	UNIT 1--
002	2	INT2--, CLK 2	MASK 2, CLK 2	UNIT 2--
003	3	INT3--, CLK 3	MASK 3, CLK 3	UNIT 3--
004	4	INT4--, CLK 4	MASK 4, CLK 4	UNIT 4--
005	5	INT5--, CLK 5	MASK 5, CLK 5	UNIT 5--
006	6	INT6--, CLK 6	MASK 6, CLK 6	KBINT--
007	7	INT7--, CLK 7	MASK 7, CLK 7	USER P15
008	8	INT8--, CLK 8	MASK 8, CLK 8	USER P14
009	9	INT9--, CLK 9	MASK 9, CLK 9	USER P13
010	10	INT10--, CLK 10	MASK 10, CLK 10	USER P12
011	11	INT11--, CLK 11	MASK 11, CLK 11	USER P11
012	12	INT12--, CLK 12	MASK 12, CLK 12	USER P10
013	13	INT13--, CLK 13	MASK 13, CLK 13	USER P9
014	14	INT14--, CLK 14	MASK 14, CLK 14	USER P8
015	15	INT15--, INTREQ--	MASK 15, RST 2	USER P7
016	16	P0 INPUT	P0 OUTPUT	USER P0
017	17	P1 INPUT	P1 OUTPUT	USER P1
018	18	P2 INPUT	P2 OUTPUT	USER P2
019	19	P3 INPUT	P3 OUTPUT	USER P3
020	20	P4 INPUT	P4 OUTPUT	USER P4
021	21	P5 INPUT	P5 OUTPUT	USER P5
022	22	P6 INPUT	P6 OUTPUT	USER P6
023	23	P7 INPUT	P7 OUTPUT	USER P7
024	24	P8 INPUT	P8 OUTPUT	USER P8
025	25	P9 INPUT	P9 OUTPUT	USER P9
026	26	P10 INPUT	P10 OUTPUT	USER P10
027	27	P11 INPUT	P11 OUTPUT	USER P11
028	28	P12 INPUT	P12 OUTPUT	USER P12
029	29	P13 INPUT	P13 OUTPUT	USER P13
030	30	P14 INPUT	P14 OUTPUT	USER P14
031	31	P15 INPUT	P15 OUTPUT	USER P15

8.6.2 SYSTEM I/O PORT

The System I/O Port occupies CRU addresses 400₁₆ through 43E₁₆ and consists of another TMS 9901 (U11) dedicated to onboard devices such as the keyboard, display, sound disc, and the audio cassette interface. Individual bit assignments for the system port are shown in Table 8-6.

8.6.2.1 Keyboard and Display Interface

Signal flow between the TMS 9901 and keyboard and display is diagrammed in Figure 8-18. UNIBUG software routines scan both the keyboard and display thereby minimizing the hardware required to drive the 80 display segments and read the 45 keyswitches.

The display is a twelve digit common cathode seven segment L.E.D. type of which the middle ten digits are used. Used digits are numbered left to right from 1 to 10. Segments within a digit are designated as shown in Figure 8-19.

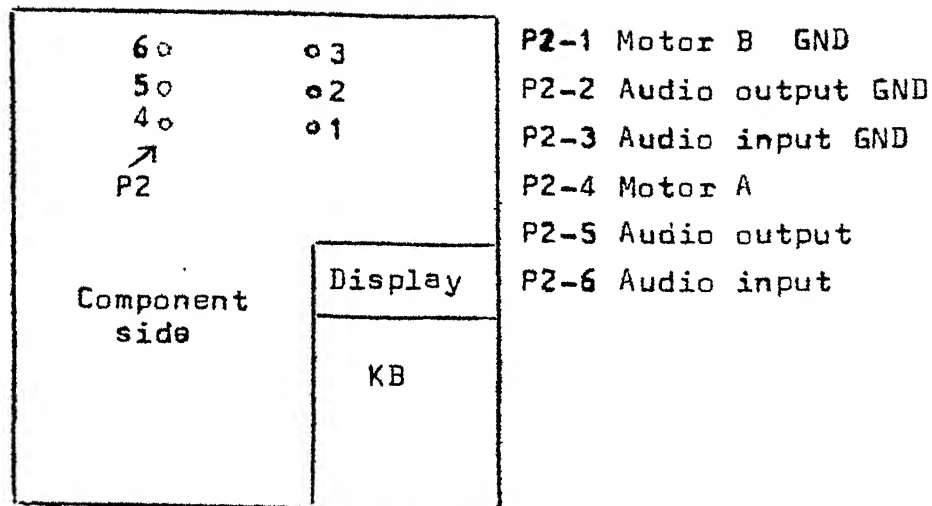


Fig 4.8(a): ACI Connector Pins

Recorder	P2 Connections
Auxiliary input	P2-5 (Audio Output) and P2-2 (GND)
Earphone Output	P2-6 (Audio Input) and P2-3 (GND)

Fig 4.8(b): Recorder And ACI Connections

provided through the Bus Expansion Interface. The system memory map, Fig 4.9, shows the organization of the memory space.

4.2 DATA ACQUISITION AND DISPLAY SYSTEM

The schemes for data acquisition and display systems are discussed in the third chapter. The details of the schemes are explained in the following paragraphs.

4.2.1 SAMPLE AND HOLD

The sample and hold chip (SHM-IC-1) [3] used is shown in Fig 4.10(a). It is a self contained device requiring only an external holding capacitor, the value of which can be chosen according to the requirements of speed and accuracy. The required unity gain, noninverting sample and hold is shown in Fig 4.10(a).

We restrict our input signal magnitude to lie between +5V and -5V. The ADC which follows the S/H needs an analog input of -5V to +5V or 0V to 10V. The 100 PF capacitor gives an acquisition time of 2 micro seconds. To eliminate offset we use a 100 K ohm trimming potentiometer.

4.2.2 ANALOG TO DIGITAL CONVERTER

The analog to digital converter (ADC-EH8B2) [3] used is shown in Fig 4.10(c). The key features of this model are a 2 micro seconds conversion time, unipolar and bipolar operation, parallel and serial outputs and its low cost.

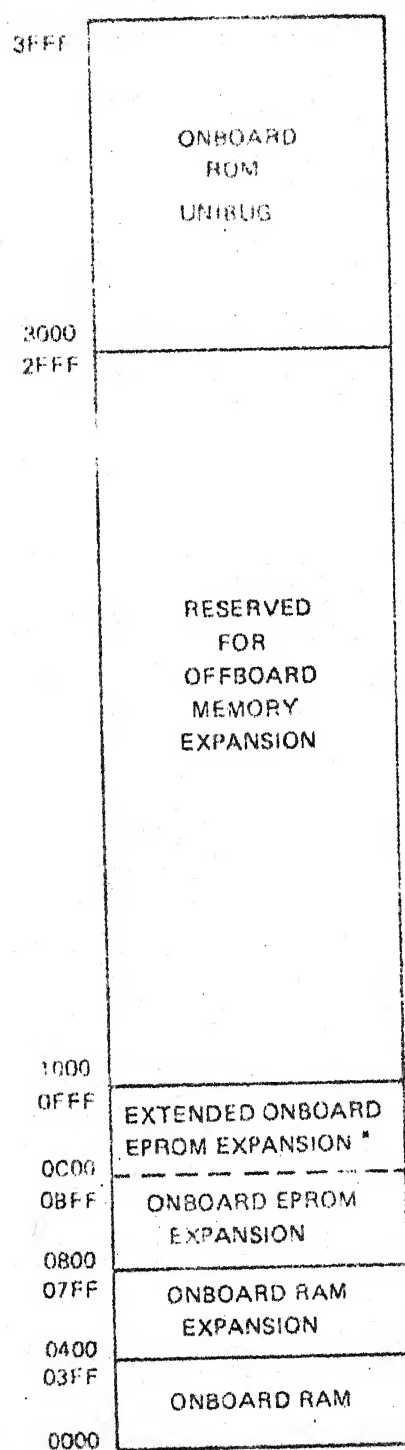


Fig 4.9: System Memory Map

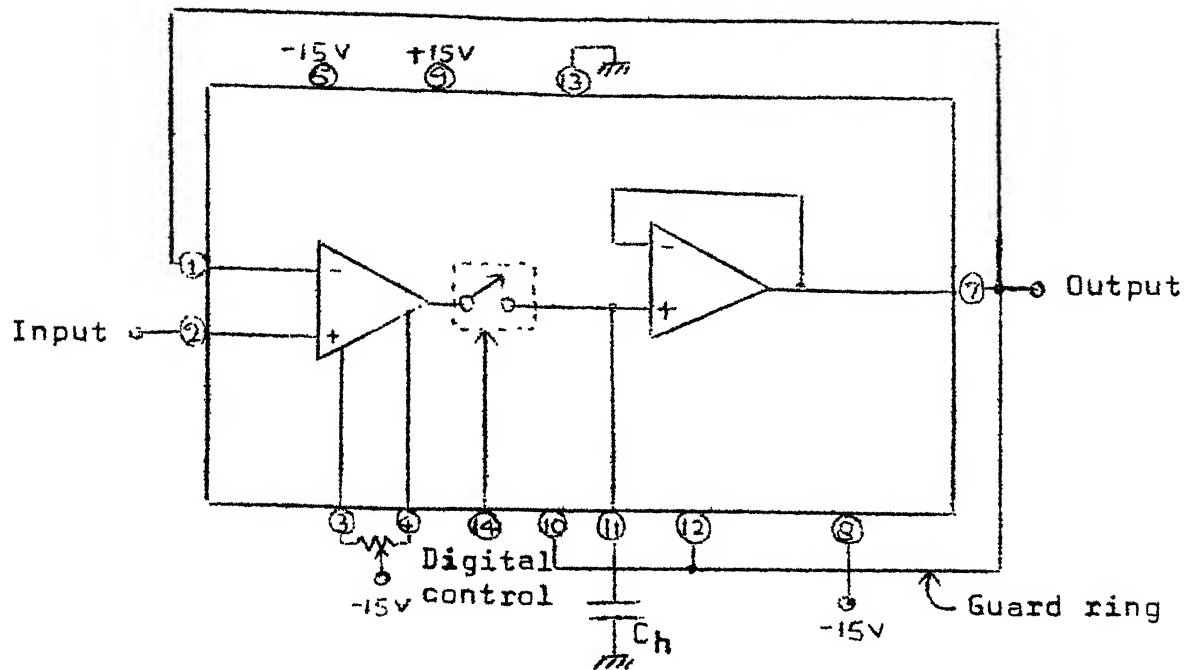


Fig 4.10(a): Model of sample-hold (SHM-IC-1)

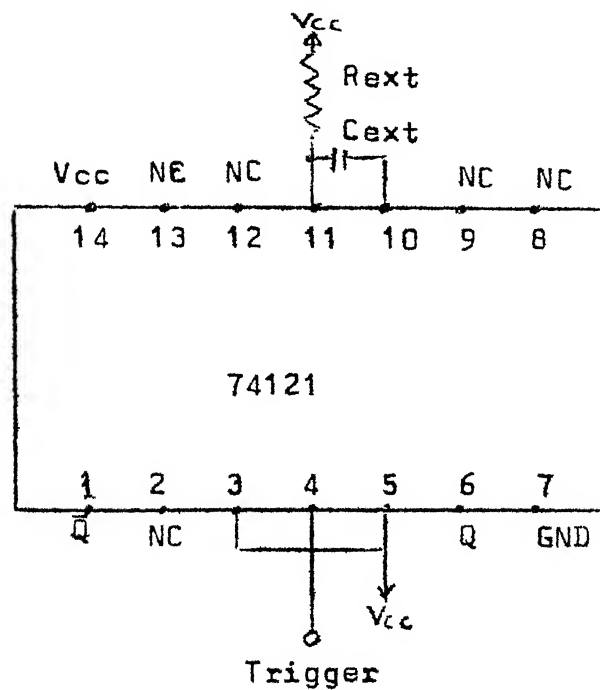


Fig 4.10(b): Pin configuration of monostable

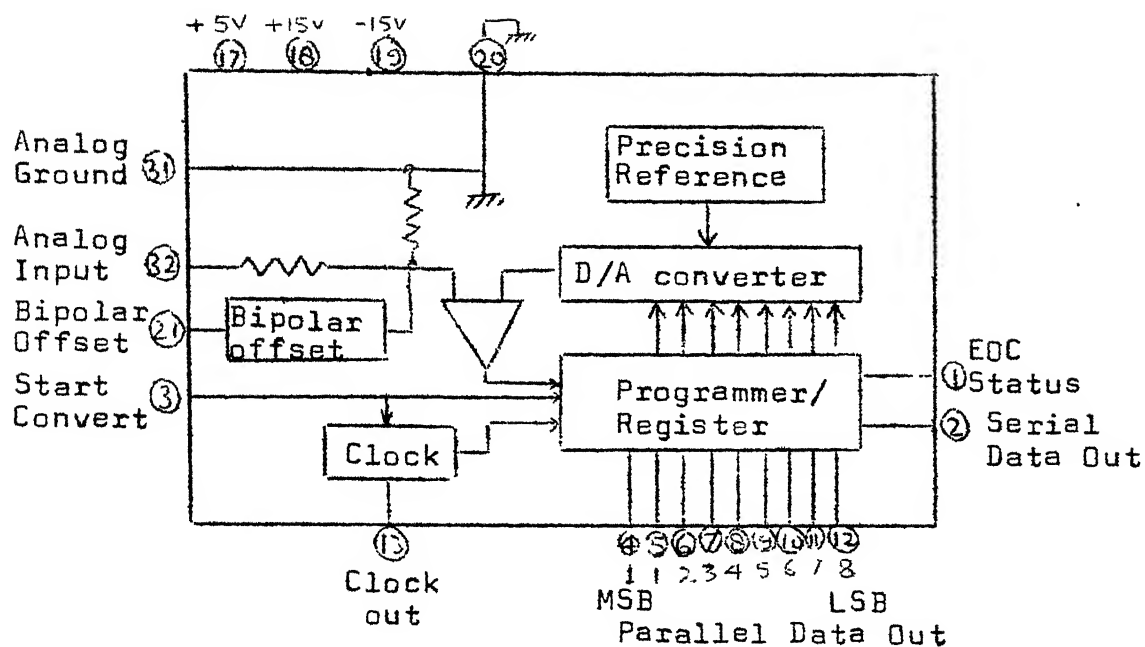


Fig 4.10(c): Model of Analog to Digital Converter (ADC-EH8B2)

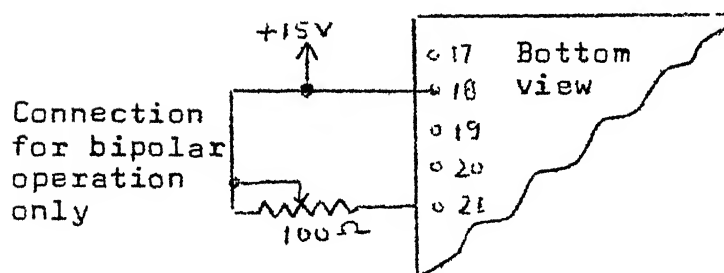


Fig 4.10(d): Bipolar operation of ADC-EH8B2

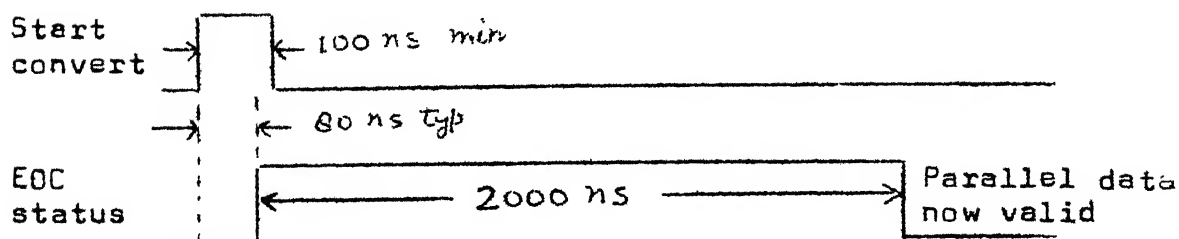


Fig 4.10(e): Timing Diagram for ADC-EH8B2

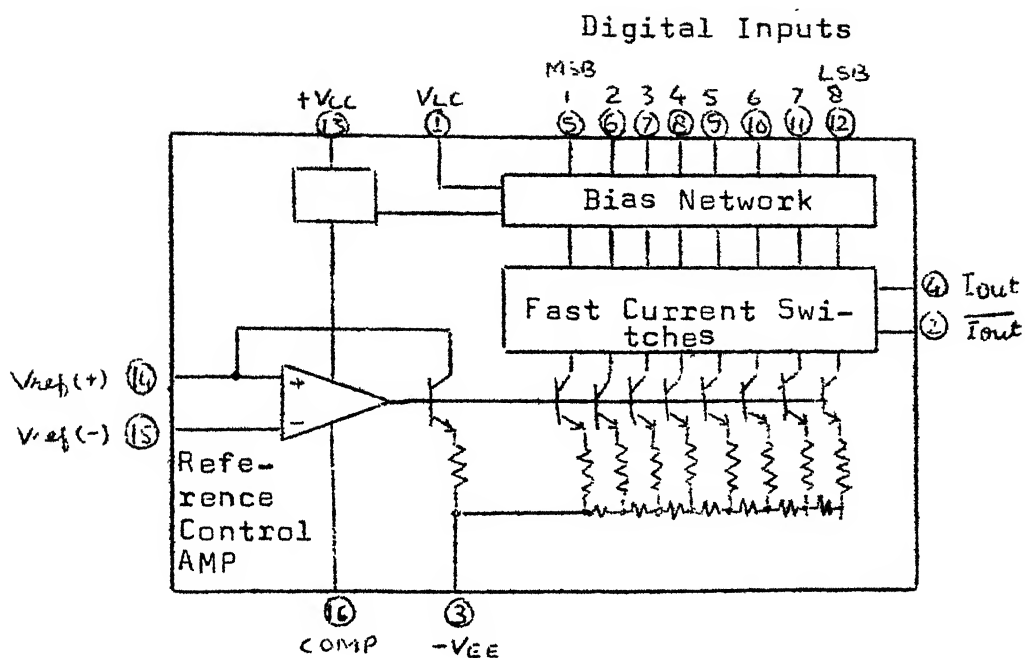


Fig 10(f): Model of Digital to Analog Converter

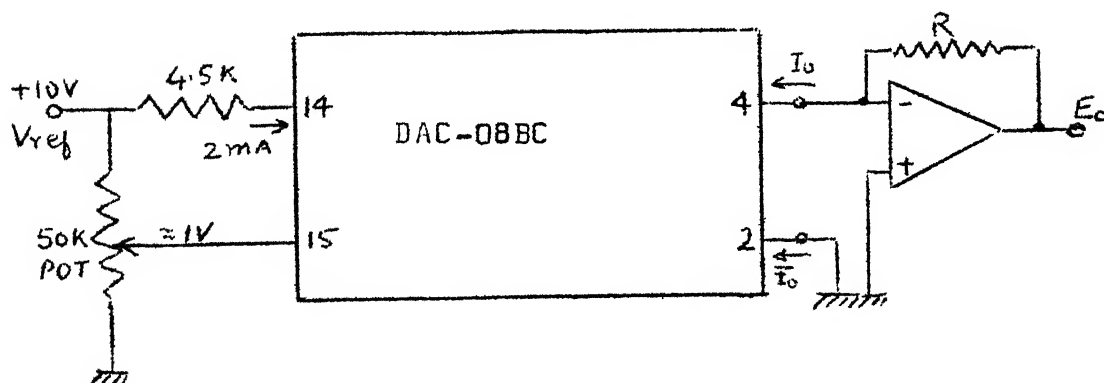


Fig 10(g): Unipolar Operation of DAC

The output can be either in 2's complement or offset binary. Since the input to ADC varies between +5V and -5V. Therefore we configured the converter to give bipolar operation. For bipolar operation calibration is necessary. We connected the +15V supply to pin 21 of the converter through a 100 ohm trimming potentiometer as shown in Fig 4.10(d). A precision voltage source is connected to pin 32 and the input voltage set to 0.020 volts. The potentiometer is adjusted such that the output code flickers equally between 10000000 and 10000001. The timing diagrams for the analog to digital converter are shown in Fig 4.10(e).

The start convert input signal to ADC is generated by monostable circuit. The configuration of the 74121 is shown in Fig 4.10(b). The output pulse is given by the formula

$$T = R_{ext} C_{ext}$$

The start convert pulse should be at least of 100 nano seconds duration. We choose the pulse width to be 200 nano seconds and

$$C_{ext} = 47 \text{ PF}$$

$$R_{ext} = 5.6 \text{ K ohm}$$

trigger pulse which generates the start convert pulse given by PSI, generated via software of the system.

4.2.3 DIGITAL TO ANALOG CONVERTER

The 8-bit digital to analog converter (DAC-08BC) [3] is shown in Fig 4.10(f). It provides very high speed of 85 nano-seconds coupled with low cost and application flexibility. For unipolar operation, the arrangement is shown in Fig 4.10(g).

CENTRAL LIBRARY
KANPUR.

Acc. No. A.....82559.....

CHAPTER 5

SOFTWARE DESIGN

Ever since the development of the first micro-processor in 1971, there has been a tremendous increase in the application of microprocessor in diverse areas such as process control, instrumentation, consumer products, data acquisition and many real time application. The micro-processors have their limitations in scientific and real time application. These limitations mainly arise because of the word length and the speed of available microprocessors.

In this chapter, we will discuss the implementation of FFT on TMS 9980A microprocessor.

5.1 SELECTION OF FIXED-POINT ARITHMETIC

We selected fixed-point arithmetic over floating point arithmetic, because fixed point is faster than floating point though less accurate. In the FFT program utilizing fixed-point arithmetic, the input sequence is scaled such that it can be represented by N bits plus sign and the binary point is assumed to lie to the left of the leftmost magnitude bit. As we move from stage to stage of the program, the magnitudes of the numbers in the sequence generally increase which may cause overflows during different stages of computations. To prevent overflows, scaling is required in fixed-point arithmetic.

5.2 SCALING [4]

The butterfly cycle of the power of two FFT algorithm operates on two complex numbers from the sequence. It takes these two numbers and produces two new complex numbers which replace the original ones in the sequence. Let $X_m(i)$ and $X_m(j)$ be the original numbers. Then, the new pair is given by

$$X_{m+1}(i) = X_m(i) + X_m(j) W^P$$

$$X_{m+1}(j) = X_m(i) - X_m(j) W^P$$

With the assumption that the binary point lies at the extreme left, the relationship among the numbers in m^{th} stage and $m+1^{\text{st}}$ stage is shown in Fig 5.1. The outside square gives the region of the possible values, $\text{Re}[X_m(i)] < 1$ and $\text{Im}[X_m(i)] < 1$. The circle inscribed in this square gives the region $|X_m(i)| < 1$. The circle inscribed in the inside square gives the region $|X_m(i)| < \frac{1}{2}$. Now if $X_m(i)$ and $X_m(j)$ are inside the smaller circle, then $X_{m+1}(i)$ and $X_{m+1}(j)$ will be inside the larger circle and hence not result in an overflow. Consequently, if we control the sequence at the m^{th} stage so that $|X_m(i)| < \frac{1}{2}$, we are certain we will have no overflow at the $m+1^{\text{st}}$ stage. However, if $X_m(i)$ and $X_m(j)$ are inside the smaller square, then it is possible for $X_{m+1}(i)$ or $X_{m+1}(j)$ to be outside the larger square and hence result in overflow.

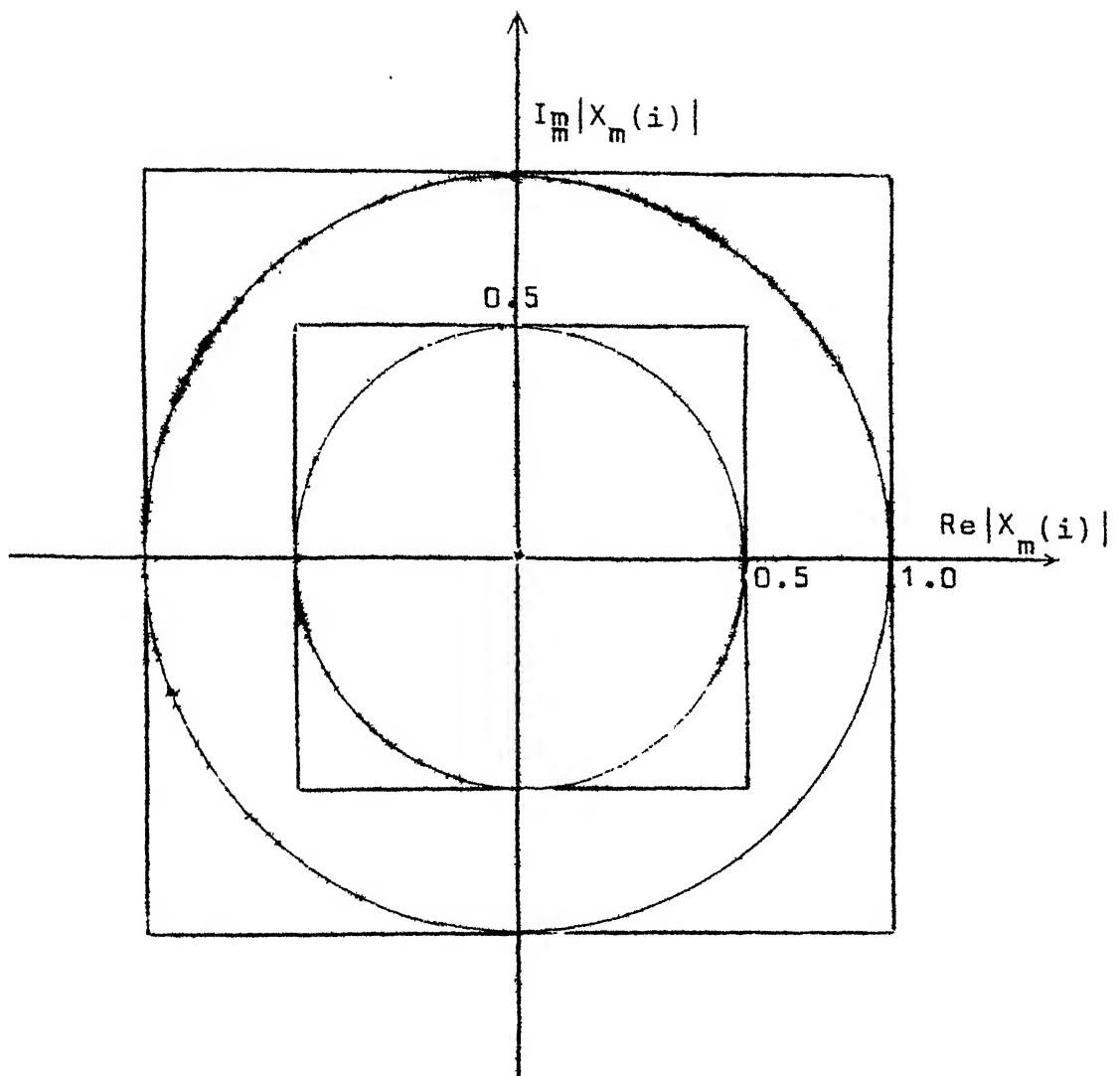


Fig 5.1: Relationship between numbers in m^{th} and $m+1^{\text{th}}$ stage.

Three techniques of scaling are given below :

(i) SHIFTING RIGHT ONE BIT AT EVERY ITERATION:

If the initial sequence $X_0(i)$, is scaled so that $|X_0(i)| < \frac{1}{2}$ for all i and if there is a right shift of one bit after every iteration, then there will be no overflow.

(ii) CONTROLLING THE SEQUENCE SO THAT $|X_m(i)| < \frac{1}{2}$

If the initial sequence is scaled so that $|X_0(i)| < \frac{1}{2}$ for all i , then at each iteration we check $|X_m(i)|$ and if it is greater than one half for any i we shift right one bit before calculation throughout the next iteration.

(iii) TESTING FOR AN OVERFLOW

In this case the initial sequence is scaled so that $\text{Re}[X_0(i)] < 1$ and $\text{Im}[X_0(i)] < 1$ whenever an overflow occurs in an iteration the entire sequence is shifted right by one bit and the iteration is continued at the point at which the overflow occurred.

The first technique is the simplest and easy to adapt for microprocessor. This method gives less accuracy than the other two techniques. In our system, the first technique has been selected.

5.3 ASSEMBLY LANGUAGE CODING OF FFT PROGRAM

The in-place algorithm is slow and requires less memory locations compared to the natural input-output algorithm. Our system has only 2048 bytes of onboard RAM. Therefore the in-place algorithm for 32 sample points has been selected for our system.

The FFT flow chart used for writing a program is shown in Fig 5.2. An assembly listing of the FFT program on the microprocessor TMS 9980A is given in Appendix-A. The details of the program is carried out in the following sections.

5.3.1 INITIALIZATION

To initialize the FFT program, we do following

No. of sample points $N = 32$

Computation array $k = 1$

Number of computation array $r = 5$

Index of the data array $K = 0$

5.3.2 WEIGHT GENERATION (W)

The values of SINE and COSINE can be generated and stored in a array before entering the FFT. For this purpose only $\frac{N}{4} + 1$ values of SINE from 0 to $\pi/2$ in a step size of $2\pi/N$ are needed and the other values of SINE and all the values of COSINE can be generated from these values. These $N/4+1$ values of SINE correspond to $N/4+1$ weights of W , i.e. $w^0, w^1, \dots, w^{N/4}$.

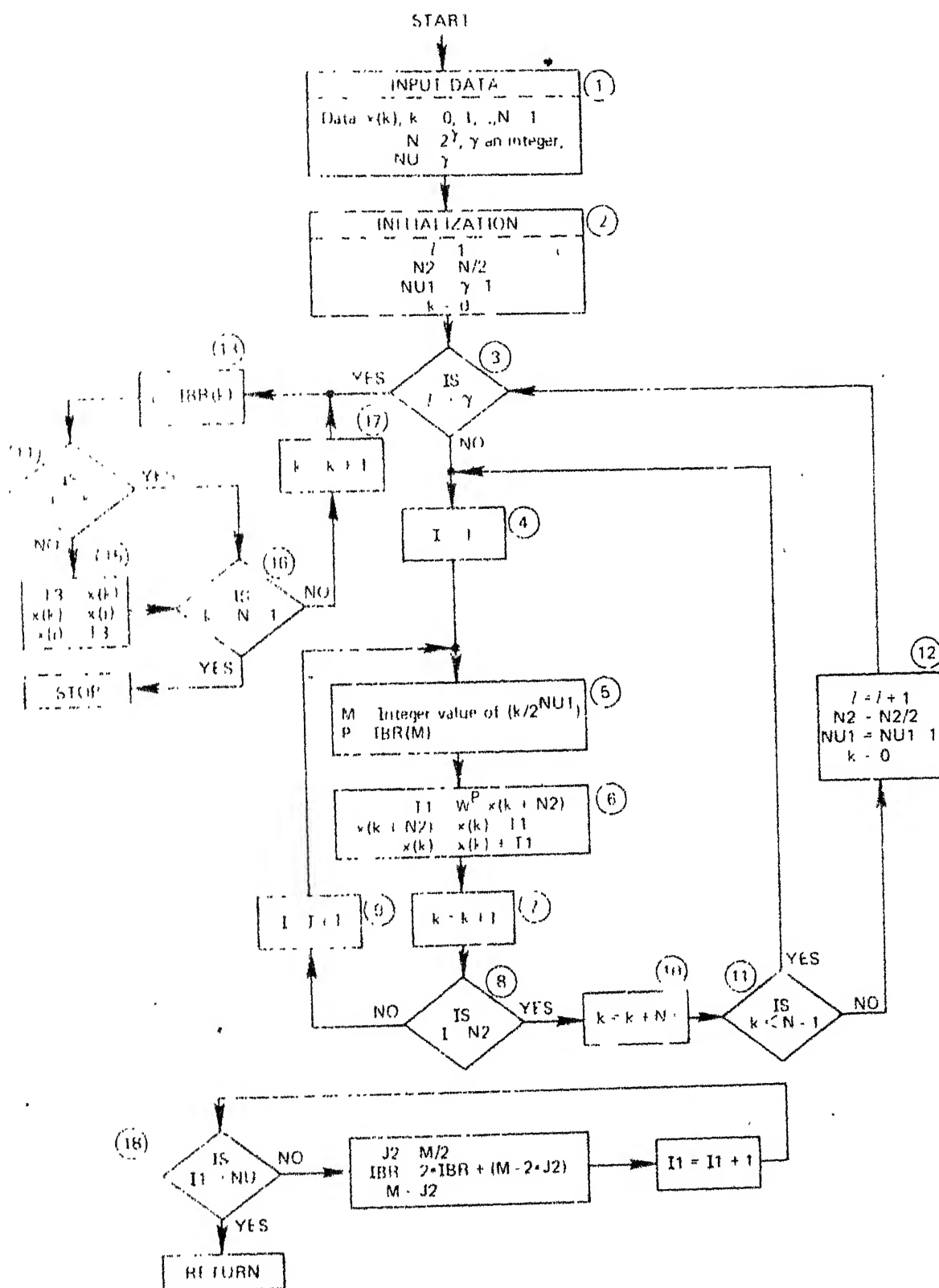


Figure 5.2: FFT computer program flow chart.

For example, for $N = 32$, 9 values of SINE are stored from 0 to $\pi/2$ in a step size of $2\pi/32$ shown in Fig 5.3. These correspond to $W^0, W^1 \dots W^8$. Taking the left most bit as sign bit and others as a mantissa, the values of SINE will vary from 0000 0000 to 0111 1111. A set of nine values in hexadecimal is given in Fig 5.3. These values are stored in the system memory (M.A.: 0500-050C) before executing the program.

Location in Memory	Argument of SINE (Radians)	Value of SINE (Hexadecimal)
0	0	0000
1	$(2\pi/32) \times 1$	18F8
2	$(2\pi/32) \times 2$	30FB
3	$(2\pi/32) \times 3$	471C
4	$(2\pi/32) \times 4$	5A82
5	$(2\pi/32) \times 5$	6A6D
6	$(2\pi/32) \times 6$	7641
7	$(2\pi/32) \times 7$	7D8A
8	$(2\pi/32) \times 8 (= \pi/2)$	7FFF

Fig 5.3: Values of SINE stored in Memory

(a) CALCULATION OF OTHER SINE VALUES ($N=32$)

For calculating the values of SINE required in the FFT program, following procedure is adopted:

(i) The program should check whether the index is

$$\leq \frac{N}{4} \text{ or } > \frac{N}{4}$$

(ii) If index $\leq \frac{N}{4}$, then use the index as it is to

fetch the appropriate value of SINE from the array.

- (iii) If index $> \frac{N}{4}$, the index is subtracted from $\frac{N}{2}$ and this value is used as the index for fetching the appropriate value of SINE.

(b) CALCULATION OF COSINE VALUES (N=32)

The following procedure is followed

- (i) The program checks whether the value of index $\leq \frac{N}{4}$ or $> \frac{N}{4}$
- (ii) If index $\leq \frac{N}{4}$, subtract the index from $\frac{N}{4}$ and use this value as index to fetch the value from SINE array
- (iii) If index $> \frac{N}{4}$, subtract $\frac{N}{4}$ from the index and use this value as the index to fetch the value from SINE array. This will give appropriate COSINE values.

The software is written to generate all the SINE and COSINE values.

5.3.3 SUBROUTINES

The subroutines which will be called by FFT program are given below :

(a) BIT-REVERSAL ROUTINE (IBR)

The flow chart for bit-reversal operation is shown

by box-18 of the Fig 5.2. The assembly program for the routine is given in Appendix-A.

(b) BUTTERFLY COMPUTATION ROUTINE

The butterfly computation pattern for 8-point FFT is illustrated in Fig 2.1. For an N-point FFT, the basic computation involves the evaluation of the following equations

$$\begin{aligned} D_1' &= D_1 + W^P D_2 \\ D_2' &= D_1 - W^P D_2 \end{aligned} \quad (5.1)$$

where $W = e^{j2\pi/N}$, P is an integer and D_1 and D_2 are complex numbers fetched from sample locations in memory. D_1' and D_2' are the new values generated by the transformation to be stored back in the same locations where D_1 and D_2 were fetched from. The computation D_1' and D_2' from D_1 and D_2 and W^P in accordance with the equation (5.1) is the butterfly computation. This involves the multiplication of two complex numbers and the various steps in the computation are shown below.

$$\begin{aligned} \text{Let } D_1 &= D_{1R} + jD_{1I} \\ D_2 &= D_{2R} + jD_{2I} \\ W^P &= X + jY \\ \text{and } W^P \cdot D_2 &= A + jB \\ \text{then } A &= X \cdot D_{2R} - Y \cdot D_{2I} \\ B &= Y \cdot D_{2R} + X \cdot D_{2I} \end{aligned}$$

- 1) Multiply D_{2R} and X , $R1 = D_{2R} \cdot X$
- 2) Multiply D_{2I} and Y , $R2 = D_{2I} \cdot Y$
- 3) Add $A = R1 - R2$
- 4) Compute $D'_{1R} = D_{1R} + A$
- 5) Compute $D'_{2R} = D_{1R} - A$
- 6) Multiply D_{2R} and Y , $R3 = D_{2R} \cdot Y$
- 7) Multiply D_{2I} and X , $R4 = D_{2I} \cdot X$
- 8) Add $B = R3 + R4$
- 9) Compute $D'_{1I} = D_{1I} + B$
- 10) Compute $D'_{2I} = D_{1I} - B$
- 11) Store D'_1 and D'_2 in place of D_1 and D_2

(c) OPTIMIZATION OF PROGRAM

For real data inputs, the algorithms discussed in the section 2.8 is more time saving than the generalized algorithm chosen for our system in which the input datas are assumed complex. Since practically our input datas are also real, therefore we tried to optimize the program by exploiting the vary nature of the chosen algorithm. There are $r(r=\log_2 N)$ iterations in the FFT program. In the first iteration, the weight of W is zero, which gives value of $X=\sin$ as zero and $Y=\cos$ as one. This means that the components in first array can be computed by simply addition and subtraction and the need for multiplication with SINE and COSINE is eliminated.

For example :

$$D'_{1R} = D_{1R} + D_{2R}$$

$$D'_{1I} = 0 \text{ (Imaginary part is zero)} \quad (5.2)$$

$$D'_{2R} = D_{1R} - D_{2R}$$

$$D'_{2I} = 0 \text{ (Imaginary part is zero)}$$

The flow chart for computing butterfly cycles is shown in Fig 5.4. The figure indicates that for second iteration, the box-1 is repeated for half of the array as weight of W is zero. For second half of the array, the weight of W equals eight which gives value of $X=\text{SIN}$ as one and $Y=\text{COS}$ as zero. This means that the remaining components of the array are computed as per the equations given in box-2.

Similarly for third, fourth and etc iterations, the box-3 is computed for any weight of W except the value of 0 and 8. The sequence of computations of box-3 is given in section 5.3.3(b).

The components of the array after computation through box-1, 2 or 3 are divided by 2 before storing back in the system memory.

The square of the magnitude of the imaginary and real parts of each output value after all computation is computed using the following expression

$$Z^2 = X^2 + Y^2$$

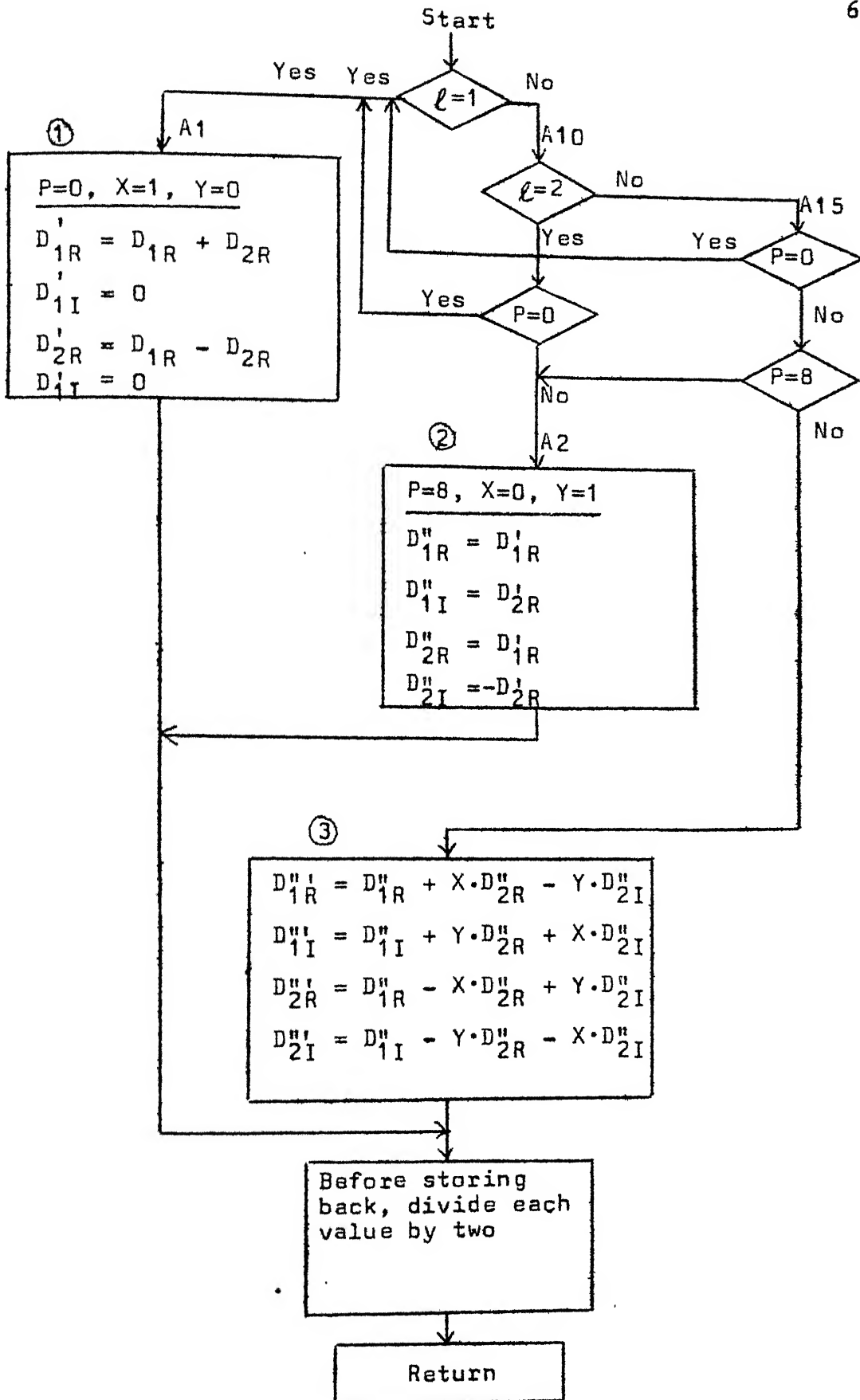


Fig 5.4: Flowchart for computing butterfly cycles

Here we are not interested in the exact value of the output, so the squares of the outputs are computed. The analog form of these values are displayed on the screen through the Z-axis of the oscilloscope.

5.3.4 SOFTWARE FOR THE DATA ACQUISITION AND THE DISPLAY SYSTEMS

The software has been developed and tested on the microcomputer for the data acquisition and the display systems. A set of instructions that have been used for writing this program is shown in Fig 4.6. The used pins of PSI are selected with the help of Table 4.1 and Table 4.2. The listing of the program is given in Appendix-A.

5.4 ROUGH ESTIMATION OF EXECUTION TIME

The rough execution time for one FFT for 32 points can be calculated by observing Fig 5.2 and the program listed in Appendix-A. We assume the average number of clock cycles for each instruction is 20 and the addressing modes are in work-space register modes [5]. The time ($t_c(\emptyset)$) for one clock cycle is 0.400 micro-seconds. The formula used to calculate the execution time (T) for one instruction is

$$T = t_c(\emptyset) (C+W \cdot M) ;$$

C = Clock cycles

M = 0 (workspace register mode)

The total time taken by butterfly routine	= 50.00 msec.
The total time taken by bit reversal routine	= 145.00 msec.
Time taken by Main program	= 15.00 msec.
Time taken by DAS	= 7.00 msec.
Time taken by Display system	= 7.00 msec.

Total time (approx.)	<u>324.00 msec.</u>
----------------------	---------------------

Hence the accuracy of FFT points is reduced due to round off error. The accuracy can be increased by using 16 bits ADCs and DACs.

The execution time to compute FFT for a set of 32 points is 324 m sec.

Our system is not made for real time computation. The system samples a set of 32 points in a period of 324 m sec, and the information contained in this period is lost. A real time system can be designed if we choose a high speed processor.

6.2 FUTURE WORK

The following related work to spectrum analysis is suggested to improve the performance:

1. The spectrum analyser for real time can be developed.
2. The off-board memory area on TM 990/189 can be used. For this purpose 74LS245 buffers are needed. At present they were not available in the store.
3. The 8086 or any other 16-bits microprocessor can be tried out in place of TMS 9980A.
4. Parallel processor organization instead of sequential scheme may be tried to exploit parallelism in the algorithm.
5. The algorithms discussed in sections 2.4 and 2.8 can be tried out.
6. The spectrum analyser can also be designed with Bit-slice microprocessors.

REFERENCES

1. Brigham, E.O., 'The Fast Fourier Transform'.
2. Rabiner and Gold, 'Theory and Applications of Digital Signal Processing'.
3. Digital Intersil "Engineering Product Handbook" (Manfield: Datel System Inc., 1979)
4. Welch, P.D., "A Fixed-Point Fast Fourier Transform Error Analysis". IEEE Trans. Audio Electroacoustics, 1969.
5. TM 990/189 Microcomputer User's Guide, Texas Instruments, Inc., July 1979.
6. 9900 Family Systems Design and Data Book Microprocessor Series, TI Inc., 1980.
7. FFT: 'Theory, Applications and Hardware' Short term course, Feb 25-March 9, 1976, Dept. of Electrical Engg., IIT Madras.
8. Chatwani, Dilip and Datar, N.N., "Microcomputer Implementation of Real-Time Computation of FFT". B.Tech. Project, April 1982.
9. Stanley, W.D., 'Digital Signal Processing', Reston Publishing Co., Inc., 1975.

APPENDIX-AASSEMBLY LISTING

Memory Address	Machine Code	Instruction	Comments

1. Nine values of SINE from 0 to $\pi/2$ in step of $2\pi/32$ stored			
07FE	18F8		
07F2	30FB		
07F4	471C		
07F6	5A82		
07F8	6A6D		
07FA	7641		
07FC	7D8A		
07FE	7FFF		
2. Initial values			
612	0005		value of r
614	0020		value of N
3. Program for data acquisition system			
0510	04CC	CLR R12	
0512	0203	LI R3, > 630	
0514	0630		
0516	04C4	CLR R4	
0518	1D00	SBO 0	clock mode
051A	1E0F	SBZ 15	all I/O becomes in input mode
051C	1E00	SBZ 0	
051E	020C	LI R12, > 0002	
0520	0002		
0522	04C4	CLR R4	
0524	3244	LDCR R4, R9	
0526	1000	NOP	
0528	1D14	SBO 20	P5=1 for ADC enable
052A	020C	LI R12, > 030	
052C	0030		
052E	1EFE	SBZ -2	
0530	020C	yy LI R12, > 030	
0532	0030		
0534	1DFE	SBO -2	clock at P6
0536	1EFE	SBZ -2	
0538	1000	NOP	
053A	04D3	CLR *R3	
053C	3613	STCR *R3, 8	
053E	05C3	INCT R3	R3=R3+2

0540	0584	INC R4
0542	0284	CI R4, 32
0544	001F	
0546	12F4	JLE >530
0548	1000	NOP
054A	1000	NOP
054C	0204	LI R4, >6F0
054E	06F0	
0550	0201	LI R1, >630
0552	0630	
0554	0200	LI R8, >8000
0556	8000	
0558	C0F1	AA2 MOV *R1+, R3
055A	2008	CDC R8, R3
055C	1303	JEQ AA0
055E	CD03	MOV R3, *R4+
0560	04F4	CLR *R4+
0562	1003	JMP AA1
0564	0503	AA0 NEG R3
0566	CD03	MOV R3, *R4+
0568	0734	SET0 *R4+
056A	04F4	AA1 CLR *R4+
056C	04F4	CLR *R4+
056E	0284	CI R4, >7F0
0570	07F0	
0572	11F2	JLT AA2
0574	1000	NOP
0576	1083	JMP >47E
047E	10D0	JMP >420
0420	10A3	JMP >368

4. Main FFT program

0368	02E0	LWPI >670	
036A	0670		
036C	0201	LI R1, 1	/ =1
036E	0001		
0370	0209	LI R9, >612	
0372	0612		
0374	C039	MOV *R9+, R0	r=5
0376	04C3	CLR R3	
0378	C143	MOV R3, R5	K0
037A	C139	MOV *R9+, R4	
037C	C184	MOV R4, R6	
037E	0606	DEC R6	R6 = N-1
0380	0914	SRL R4, 1	N2 = N/2 = 16
0382	CE44	MOV R4, *R9+	N2, MA=616
0384	0600	DEC R0	r=1=NU1
0386	8801	L1 C R1, @ >612	r
0388	0612		
038A	151E	JGT LY	

038C	0202	L2 LI R2, 1	R2=I=1
038E	0001		
0390	C0C5	L3 MOV R5, R3	R3=K
0392	0280		
0394	0000	CI R0, 0	
0396	1301	JEQ A1	
0398	0903	SRL R3, 0	$M = \frac{K}{2^{NU1}}$
039A	C803	A1 MOV R3, @ > 6B2	
039C	06B2		
039E	0420	BLWP @ > 340	
03A0	0340		
03A2	0420	BLWP @ > 150	Butterfly
03A4	0150		
03A6	0585	INC R5	K=K+1
03A8	C285	MOV R5, R10	K → R10
03AA	8102	C R2, R4	I=N2
03AC	1302	JEQ L20	
03AE	0582	INC R2	I=I+1
03B0	10EF	JMP L3	
03B2	A284	L20 A R4, R10	K=K+N2
03B4	C14A	MOV R10, R5	
03B6	018A	C R10, R6	K < N-1
03B8	11E9	JLT L2	
03BA	04C5	CLR R5	K=0
03BC	0600	DEC R0	NU1-1
03BE	0914	SRL R4, 1	
03C0	C804	MOV R4, @ > 616	N2=N2/2
03C2	0616		
03C4	0581	INC R1	Q=Q+1
03C6	10DF	JMP L1	
03C3	C805	LY MOV R5, @ > 6B2	
03CA	06B2		
03CC	0420	BLWP @ > 340	i = IBR(K)
03CE	0340		
03D0	C1E0	MOV @ > 61C, R7	i → R7
03D2	061C		
03D4	8147	C R5, R7	i ≤ K
03D6	121A	JLE L2	
03D8	C285	MOV R5, R10	R5=R10=K
03DA	0A3A	SLA R10, 3	8K
03DC	0209	LI R9, > 6F0	Addr. of X(K)
03DE	06F0		
03E0	A289	A R9, R10	(6F0+8K) → R10
03E2	C03A	MOV *R10+, R0)	
03E4	C07A	MOV *R10+, R1)	T3 ← X(K)
03E6	C0FA	MOV *R10+, R3)	
03E8	C11A	MOV *R10, R4)	
03EA	C207	MOV R7, R8	i → R8
03EC	0A38	SLA R8, 3	
03EE	A209	A R9, R8	(8i+6F0) → R8
03F0	064A	DECT R10	
03F2	064A	DECT R10	

03F4	064A	DECT R10	
03F6	CEB8	MOV *R8+, *R10+	
03F8	CEB8	MOV *R8+, *R10+	
03FA	CEB8	MOV *R8+, *R10+	
03FC	C698	MOV *R8, *R10	
03FE	0648	DECT R8	
0400	0648	DECT R8	
0402	0648	DECT R8	
0404	CE00	MOV R0, *R8+	$X(i) \leftarrow T3$
0406	CE01	MOV R1, *R8+	Unscrambled values
0408	CE03	MOV R3, *R8+	
040A	C604	MOV R4, "R8	
040C	8185	LZ C, R5, R6	
040E	1302	JEQ LP	
0410	0585	INC R5	
0412	10DA	JMPY	
0414	1000	LP NOP	

5. Program for display system.

0416	0201	LI R1, >6F0	
0418	06F0		
041A	0205	LI R5, >630	
041C	0630		
041E	1001	JMP \$+4	
0420	10A3	JMP 368	
0422	COB1	AO MOV *R1+, R2	
0424	1000	NOP	
0426	CO02	MOV R2, R0	
0428	3880	MPY R0, R2	x^2
042A	05C1	INCT R1	
042C	COF1	MOV *R1+, R3	
042E	1000	NOP	
0430	CO03	MOV R3, R0	
0432	1002	JMP >438	
0434	1031	JMP >498	
0436	1080	JMP >338	
0438	38C0	MPY R0, R3	y^2
043A	A083	A R3, R2	$z^2 = x^2 + y^2$
043C	0A22	SLA R2, 2	
043E	CB42	MOV R2, *R5+	
0440	05C1	INCT R1	
0442	0281	CI R1, >7F0	
0444	07F0		
0446	11EE	JLT AO	
0448	1000	NOP	
044A	1000	CO NOP	
044C	0203	LI R3, >630	
044E	0630		
0450	04C4	CLR R4	
0452	020C	LI P12, >02A	

0454	002A		
0456	1E00	SBZ	
0458	1000	NOP	
045A	020C	LI R12, >030	P5=0 enable display system
045C	0030		
045E	1EFE	SBZ -2	
0460	020C	YY LI R12, >030	
0462	0030		
0464	1DFE	SBZ -2	clock at P6
0466	1EFE	SBZ -2	
0468	1000	NOP	
046A	3213	LDCR *R3, 8	
046C	05C3	INCT R3	
046E	0584	INC R4	
0470	0284	CI R4, 32	
0472	0020		
0474	12F5	JLE >460	
0476	1000	NOP	
0478	1000	NOP	
047A	104A	JMP >510	

6. Sub-routine for Butterfly cycles.

0150	0690	LWPI >690	
0152	0154		
0154	C060	MOV @ >67A, R1	R1=K
0156	067A		
0158	C0C1	MOV R1, R3	
015A	0A31	SLA R1, 3	
015C	1000	JMP \$+2	
015E	0202	LI R2, >6F0	
0160	06F0		
0162	A042	A R2, R1	R1=6F0+8K addr. of D1
0164	A0E0	A @ >616, R3	K+N2
0166	0616		
0168	0A33	SLA R3, 3	
016A	A0C2	A R2, R3	6F0+8(K+N2)= addr. of D2
016C	0202	LI R2, >7F0	addr. of W ^P
016E	07F0		
0170	C2A0	MOV @ >672, R10	R10=ℓ
0172	0672		
0174	028A	CI R10, 1	ℓ=1
0176	0001		
0178	162A	JNE A10	
017A	C131	A1 MOV *R1+, R4	
017C	C191	MOV *R1, R6	Sign of D _{1R}
017E	0208	LI R8, >8000	
0180	8000		
0182	2188	COC R8, R6	
0184	1601	JNE B1	If sign is +ve

0186	0504	NEG R4	
0188	C173	B1 MOV *R3+, R5	D2R
018A	C093	MOV *R3, R2	Sign of D ₂ R
018C	2088	COC R8, R2	
018E	1601	JNE B2	
0190	0505	NEG R5	
0192	C1C4	B2 MOV R4, R7	D1R
0194	020A	LI R10, >6B2	
0196	06B2		
0198	CE87	MOV R7, *R10+	
019A	CE85	MOV R5, *R10+	
019C	CE85	MOV R5, *R10+	
019E	C684	MOV R4, *R10	
01A0	0420	BLWP @ >4C6	
01A2	04C6		To addition routine
01A4	C460	MOV @ >6BC, *R1	
01A6	06BC		
01A8	C4E0	MOV @ >6BA, *R3	
01AA	06BA		
01AC	C120	MOV @ >6B8, R4	
01AE	06B8		
01B0	C1E0	MOV @ >6B2, R7	
01B2	06B2		
01B4	0914	SRL R4, 1	
01B6	0917	SRL R7, 1	
01B8	0641	DECT R1	
01BA	0643	DECT R3	
01BC	C444	MOV R4, *R1	
01BE	C4C7	MOV R7, *R3	
01C0	0380	RTWP	
01C2	028A	A10 CI R10, 2	
01C4	0002		
01C6	161A	JNE A15	
01C8	C2A0	MOV @ >61C, R10	
01CA	061C		
01CC	028A	CI R10, 0	
01CE	0000		
01D0	13D4	JEQ A1	
01D2	C131	MOV *R1+, R4	D ₁ R
01D4	0914	SRL R4, 1	
01D6	05C1		
01D8	C173	MOV *R3+, R5	D ₂ R
01DA	0915	SRL R5, 1	
01DC	CC45	MOV R5, *R1+	D ₁ i
01DE	C453	MOV *R3, *R1	
01E0	0551	INV *R1	
01E2	C2B3	MOV *R3+, R10	
01E4	CCC5	MOV R5, *R3+	D ₂ i
01E6	C4CA	MOV R10, *R3	
01E8	0641	DECT R1	
01EA	0641	DECT R1	

01EC	0643	DECT R3	
01EE	0643	DECT R3	
01F0	C4D1	MOV *R1, *R3	Sign of D_{2R}''
01F2	0641	DECT R1	
01F4	0643	DECT R3	
01F6	C4C4	MOV R4, *R3	D_{2R}''
01F8	C444	MOV R4, *R1	D_{1R}''
01FA	0380	RTWP	
01FC	C2A0	A15 MOV @ >61C, R10	
01FE	061C		
0200	028A	CI R10, 0	
0202	0000		
0204	13BA	JEQ A1	P=0
0206	028A	CI R10, 8	
0208	0008		
020A	13E3	JEQ A2	P=8
020C	1567	JGT A20	P > 8
020E	0209	LI R9, 8	
0210	0008		
0212	624A	S R10, R9	(N/4-Index) Addr. for COS value
0214	0609	DEC R9	
0216	0A19	SLA R9, 1	
0218	A242	A R2, R9	Addr. of X=COS
021A	C119	MOV *R9, R4	
021C	3913	MPY *R3, R4	$D_{2R} \cdot X$
021E	0A14	SLA R4, 1	
0220	060A	DEC R10	
0222	0A1A	SLA R10, 1	
0224	A282	A R2, R10	Addr. of Y=SIN
0226	C15A	MOV *R10, R5	
0228	3973	MPY *R3+, R5	$D_{2R} \cdot Y$
022A	0A15	SLA R5, 1	
022C	05C3	INCT R3	
022E	C19A	MOV *R10, R6	
0230	3993	MPY *R3, R6	$D_{2I} \cdot Y$
0232	0A16	SLA R6, 1	
0234	C1D9	MOV *R9, R7	
0236	39F3	MPY *R3+, R7	$D_{2I} \cdot X$
0238	0A17	SLA R7, 1	
023A	0208	LI R8, >8000	
023C	8000		
023E	C253	MOV *R3, R9	Sign of D_{2I}
0240	2248	COC R8, R9	
0242	1602	JNE A30	
0244	0506	NEG R6	
0246	0507	NEG R7	
0248	0643	A30 DECT R3	
024A	0643	DECT R3	
024C	C253	MOV *R3, R9	Sign of D_{2R}
024E	2248	COC R8, R9	

0250	1602	JNE A31	
0252	0504	NEG R4	
0254	0505	NEG R5	
0256	106F	JMP >336	
0336	107E	JMP >434	
0434	1031	JMP >498	
0498	21C8	COC R8, R7	
049A	1602	JNE B1	
049C	2148	COC R8, R5	
049E	1602	JNE B2	
04A0	61C5	B1 S R5, R7	
04A2	1003	JMP B3	
04A4	0507	B2 NEG R7	
04A6	A1C5	A R5, R7	
04A8	0507	NEG R7	
04AA	2108	B3 COC R8, R4	
04AC	1602	JNE B4	
04AE	2188	COC R8, R6	
04B0	1302	JEQ B6	
04B2	A106	B4 A R6, R4	
04B4	1003	JMP B8	
04B6	0504	B6 NEG R4	
04B8	6106	S R6, R4	
04BA	0504	NEG R4	
04BC	C284	B8 MOV R4, R10	
04BE	C147	MOV R7, R5	
04C0	10BA	JMP >436	
0436	10C0	JMP >338	
0338	1092	JMP >25E	
025E	C1B1	A90 MOV *R1+, R6	D1R
0260	C251	MOV *R1, R9	Sign of D1R
0262	2248	COC R8, R9	
0264	1601	JNE A50	
0266	0506	NEG R6	
0268	0207	LI R7, >6B2	
026A	06B2		
026C	CDC6	MOV R6, *R7+	
026E	CDCA	MOV R10, *R7+	
0270	CDC6	MOV R6, *R7+	
0272	C5C4	MOV R4, *R7	
0274	0420	BLWP @ >4C0	Addition routine
0276	04C6		
0278	C1A0	MOV @ >6B2, R6	
027A	06B2		
027C	C120	MOV @ >6B8, R4	
027E	06B8		
0280	C460	MOV @ >6BC, *R1	Sign of D1R
0282	06BC		

0284	0641	DECT R1	
0286	0914	SRL R4, 1	
0288	CC44	MOV R4, *R1+	D ₁ R
028A	C4E0	MOV @ >6BA, *R3	Sign of D ₂ R
028C	06BA		
028E	0643	DECT R3	
0290	0916	SRL R6, 1	
0292	CCC6	MOV R6, *R3+	D ₂ R
0294	1002	JMP >29A	
0296	1000	NOP	
0298	1000	NOP	
029A	05C1	INCT R1	
029C	C1B1	MOV *R1+, R6	
029E	C251	MOV *R1, R9	
02A0	2248	COC R8, R9	
02A2	1601	JNE A60	
02A4	0506	NEG R6	
02A6	C285	A60 MOV R5, R10	
02A8	0207	LI R7, >6B2	
02AA	06B2		
02AC	CDC6	MOV R6, *R7+	
02AE	CDCA	MOV R10, *R7+	
02B0	CDC6	MOV R6, *R7+	
02B2	C5C5	MOV R5, *R7	
02B4	0420	BLWP @ >4C6	
02B6	04C6		
02B8	C1A0	MOV @ >6B2, R6	
02BA	06B2		
02BC	C160	MOV @ >6B8, R5	
02BE	06B8		
02C0	C460	MOV @ >6BC, *R1	Sign of D ₁ R
02C2	06BC		
02C4	0641	DECT R1	
02C6	0915	SRL R5, 1	
02C8	C445	MOV R5, *R1	D ₁ I
02CA	05C3	INCT R3	
02CC	0916	SRL R6, 1	
02CE	CCC6	MOV R6, *R3+	D ₂ I
02D0	C4E0	MOV @ >6BA, *R3	Sign of D ₂ I
02D2	06BA		
02D4	1000	NOP	
02D6	0380	RTWP	
02D8	1000	NOP	
02DA	1000	NOP	
02DC	0209	A20 LI R9, 16	
02DE	0010		
02E0	624A	S R10, R9	(N/2-Index) Addr, for SIN values (Y)

02E2	0609	DEC R9	
02E4	0A19	SLA R9, 1	
02E6	A242	A R2, R9	Addr. of SIN (Y)
02E8	0200	LI R0, 8	
02EA	0008		
02EC	6280	S R0, R10	(Index-N/4)
02EE	060A	DEC R10	
02F0	0A1A	SLA R10, 1	
02F2	A282	A R2, R10	Addr. of COS=X
02F4	1000	NOP	
02F6	C11A	MOV *R10, R4	
02F8	3913	MPY *R3, R4	D _{2R} .X
02FA	0A14	SLA R4, 1	
02FC	C159	MOV *R9, R5	
02FE	3973	MPY *R3+, R5	D _{2R} .Y
0300	0A15	SLA R5, 1	
0302	C199	MOV *R9, R6	
0304	05C3	INCT R3	
0306	3993	MPY *R3, R6	D _{2I} .Y
0308	0A16	SLA R6, 1	
030A	C1DA	MOV *R10, R7	
030C	39F3	MPY *R3, R7	D _{2I} .X
030E	0A17	SLA R7, 1	
0310	0208	LI R8, >8000	
0312	8000		
0314	0553	INV *R3	
0316	C253	MOV *R3, R9	
0318	2248	COC R8, R9	
031A	1602	JNE A75	
031C	0507	NEG R7	
031E	1001	JMP A76	
0320	0506	A75 NEG R6	
0322	0643	A76 DECT R3	
0324	0643	DECT R3	
0326	0553	INV *R3	
0328	C253	MOV *R3, R9	
032A	2248	COC R8, R9	
032C	1602	JNE A77	
032E	0504	NEG R4	
0330	1001	JMP A78	
0332	0505	A77 NEG R5	
0334	1090	JMP A31	

7. Sub-routine for Addition and Substraction.

04C6	06B0	LWPI >6B0
04C8	04CA	
04CA	0208	LI R8, >8000
04CC	8000	
04CE	2048	COC R8, R1

04D0	1604	JNE B1
04D2	2088	COC R8, R2
04D4	1609	JNE B2
04D6	6042	S R2, R1
04D8	1001	JMP A1
04DA	6042	B1 S R2, R1
04DC	2048	A1 COC R8, R1
04DE	1602	JNE A2
04E0	0501	NEG R1
04E2	0705	SETO R5
04E4	04C5	A2 CLR R5
04E6	1003	JMP B3
04E8	0501	B2 NEG R1
04EA	A042	A R2, R1
04EC	0705	SETO R5
04EE	2108	B3 COC R8, R4
04F0	1606	JNE B4
04F2	20C8	COC R8, R3
04F4	1606	JNE B5
04F6	0504	NEG R4
04F8	6103	S R3, R4
04FA	0706	SETO R6
04FC	1008	JMP B6
04FE	A103	B4 A R3, R4
0500	1001	JMP A3
0502	A103	B5 A R3, R4
0504	2108	A3 COC R8, R4
0506	1602	JNE A4
0508	0504	NEG R4
050A	0706	SETO R6
050C	04C6	CLR R6
050E	0380	RTWP

8. Sub-routine for Bit reverse (IBR).

0340	06B0	LWPI > 6B0	
0342	0344		
0344	0206	LI R6, 1	I1=1
0346	0001		
0348	04C7	CLR R7	IBR=0
034A	C081	L9 MOV R1, R2	R1=M=J1
034C	0912	SRL R2, 1	
034E	C242	MOV R2, R9	
0350	0A19	SLA R9, 1	2.J2
0352	0A17	SLA R7, 1	2.IBR
0354	6042	S R9, R1	
0356	A1C1	A R1, R7	
0358	C042	MOV R2, R1	
035A	0586	INC R6	
035C	8806	C @>612, R6	I1 ≤ r
035E	0612		
0360	12F4	JLE L9	
0362	C807	MOV R7, @ > 61C	P=61C
0364	061C		
0366	0380	RTWP	